RECEIVED
LAWRENCE
RADIATION LABORATORY

UCRL-20567 c.2

LIBRARY AND
DOCUMENTS SECTION

# HIGH TEMPERATURE MECHANICAL BEHAVIOR OF $MgO-CaO \cdot MgO \cdot SiO_2$ MATERIALS

William E. Snowden
(M. S. Thesis)

June 1971

AEC Contract No. W-7405-eng-48

TWO-WEEK LOAN COPY

This is a Library Circulating Copy
which may be borrowed for two weeks.
For a personal retention copy, call
Tech. Info. Division, Ext. 5545

UCRL-20567 c.2

25

## DISCLAIMER

This document was prepared as an account of work sponsored by the United States Government. While this document is believed to contain correct information, neither the United States Government nor any agency thereof, nor the Regents of the University of California, nor any of their employees, makes any warranty, express or implied, or assumes any legal responsibility for the accuracy, completeness, or usefulness of any information, apparatus, product, or process disclosed, or represents that its use would not infringe privately owned rights. Reference herein to any specific commercial product, process, or service by its trade name, trademark, manufacturer, or otherwise, does not necessarily constitute or imply its endorsement, recommendation, or favoring by the United States Government or any agency thereof, or the Regents of the University of California. The views and opinions of authors expressed herein do not necessarily state or reflect those of the United States Government or any agency thereof or the Regents of the University of California.

TABLE OF CONTENTS

| | | Page |
|---|---|---|
| ABSTRACT | | v |
| I. | INTRODUCTION | 1 |
| II. | THEORY AND LITERATURE SURVEY | 3 |
| | A. Stress-Strain Behavior | 3 |
| | B. Creep | 5 |
| | C. Deformation in More Complex Systems | 11 |
| III. | EXPERIMENTAL PROCEDURE | 13 |
| | A. Specimen Preparation | 13 |
| | B. Specimen Characterization | 15 |
| | C. Mechanical Testing | 16 |
| IV. | RESULTS AND DISCUSSION | 19 |
| | A. Specimen Characterization | 19 |
| | B. Stress-Strain Tests | 29 |
| | C. Creep | 52 |
| V. | SUMMARY AND CONCLUSIONS | 65 |
| ACKNOWLEDGMENTS | | 68 |
| APPENDIX | | 69 |
| REFERENCES | | 71 |



# HIGH TEMPERATURE MECHANICAL BEHAVIOR OF $MgO-CaO{\cdot}MgO{\cdot}SiO_2$ MATERIALS

William E. Snowden

Inorganic Materials Research Division, Lawrence Radiation Laboratory, and Department of Materials Science and Engineering, College of Engineering, University of California, Berkeley, California

## ABSTRACT

The mechanical behavior of polycrystalline MgO containing small amounts of $CaO{\cdot}MgO{\cdot}SiO_2$ was studied in compression over the temperature range 1200°-1450°C. The behavior observed in stress-strain tests was related to the degree of distribution of the silicate phase, and to the temperature. From creep experiments it was determined that deformation at 1200°C was due to the motion of dislocations within the MgO grains, while at higher temperatures deformation was controlled by viscous flow of the boundary phase.

The dependence of the creep rate on stress and temperature was determined by evaluating the stress exponent and apparent activation energy for creep. The stress exponent was found to decrease from a value of 3.6 at 1200°C to a value of 1.1 at 1450°C, indicating that changes in the mechanism controlling deformation occurred as the temperature was increased. Over the same range of temperatures the apparent activation energy for creep was found to increase from 104 kcal/mole to 240 kcal/mole. Where two creep mechanisms having different activation energies are known to operate, an increase in the apparent activation energy for creep as the temperature is increased has been predicted.

# I. INTRODUCTION

Selected ceramic materials have traditionally found extensive use in applications where strength and durability at high temperatures are critical. The brittle nature of most of these materials, however, has precluded their use under load at high temperatures where the possibility of catastrophic failure is increased. In such instances some controlled amount of ductility is desirable. Consequently, viscous flow, plastic deformation, and creep are all major criteria for structural applications of ceramics at high temperatures.

While varying amounts of ductility have been observed in a number of single phase ceramic materials, the failure of most of these materials to satisfy the von Mises condition that five independent slip systems must be operative to produce a general state of deformation in polycrystals prevents much yielding. However, a significant degree of plastic flow has been observed in cubic ionic single crystals at room temperature, particularly MgO, as well as in polycrystalline material at higher temperatures where the stress levels required to activate the various slip systems are reduced. At these higher temperatures stress-induced climb and high dislocation mobility inhibit cleavage fracture, and ductility is enhanced. The contributions of other deformation mechanisms may be equally important at high temperatures as well.

The high temperature mechanical behavior of single crystal and polycrystalline MgO has been investigated in considerable detail. However, the effects of a second phase on the mechanical properties at high temperatures remain unreported. While the deformation characteristics of a number of practical refractory systems have been investigated, the systems studied were generally too complex to provide fundamental explanation of the particular deformation mechanisms involved.



The principal purpose of this work was to develop a model system, consisting of $CaO \cdot MgO \cdot SiO_2$ and MgO, which was used to study the effects of a second phase, amount and nature of distribution, on the high temperature mechanical behavior of MgO materials. The objective of the investigation was to increase understanding of the stress-strain and creep behavior of practical, more complex systems at elevated temperatures.

## II. THEORY AND LITERATURE SURVEY

### A. Stress-Strain Behavior

The mechanical behavior of MgO single crystals has been the subject of a number of investigations.[1-8] Testing has been accomplished in tension, transverse bending, and compression. In all of these studies, the behavior of MgO single crystals was related to the relative ease of dislocation movement at various temperatures. Effects of strain hardening were considered. It was also determined that the presence of impurities and environmental effects play a major role in determining whether a crystal will be brittle or ductile.[2] Increasing impurity concentration increased strength but reduced ductility as the impurities acted as barriers to dislocation motion.[6]

While the mechanical behavior of single crystal MgO can be described solely through consideration of dislocation effects, the mechanical behavior of polycrystalline MgO at high temperatures is more difficult to predict due to various other deformation mechanisms which may operate in polycrystals. In addition to dislocation mechanisms such as dislocation glide and climb, deformation may be significantly influenced by grain boundary migration, by the stress directed diffusion of vacancies either through the crystal lattice or along grain boundaries, by grain boundary sliding or by grain boundary separation. The behavior of polycrystalline material is further complicated by wide variations in microstructural features such as amount and distribution of impurities, total porosity, pore size and distribution, grain size and shape, and grain boundary characteristics. Thus material characterization is most important in attempting to determine the dominant deformation mechanism in polycrystalline MgO.



The mechanical behavior of polycrystalline MgO at elevated temperatures has been extensively studied under various conditions. A number of investigators[9-13] have obtained results from stress-strain tests and have related variations in yield stress, ductility, fracture mode, and strength at fracture to specific microstructural features in attempts to determine the predominant deformation mechanism. Stokes and Li[9] attributed the behavior of polycrystalline MgO tested in tension to the availability of mobile dislocation sources and concluded that a mere change in grain size did not in itself affect ductility. Vasilos et al.[10] studied the load vs. deflection characteristics of polycrystalline MgO tested in transverse bending and concluded that a dislocation mechanism was responsible for deformation at high temperatures. That deformation occurs by dislocation glide and climb for recrystallized and hot-pressed magnesia has also been reported by Day and Stokes,[11] although the effects of grain boundary sliding due to porosity were noted. Copley and Pask[12a] studied the stress-strain behavior of five types of polycrystalline MgO in compression at temperatures up to 1400°C. They concluded that ductility is possible in compression provided that slip can be initiated homogeneously, the resistance to dislocation motion is not too great, and the grain boundaries are sufficiently strong to resist separation or shearing. Langdon and Pask[12b] extended these studies on polycrystalline MgO and emphasized the importance of the nature of the pore structure and grain boundary impurities to the stress-strain behavior of the specimens. Finally, Evans et al.[13] studied the strength in bending of polycrystalline MgO and concluded that fracture was initiated by plastic flow over a wide range of temperatures, but that above 1300°C the fracture process was complicated by the onset of grain boundary migration.

## B. Creep

While tests of short duration have been useful in studying the mechanical behavior of polycrystalline MgO, most of the reported investigations of high-temperature deformation involve the behavior of specimens in creep. A number of models which describe material deformation occurring as a result of any of the processes mentioned previously have been proposed. Comparison of experimental data with predictions arising from these models is generally made to determine the predominant deformation mechanism during creep. Before the results of such studies on polycrystalline MgO are discussed, a brief review of creep theory will be presented.

### 1. Creep Theory

"Creep" may be defined as the time-dependent plastic flow which occurs in a material subjected to a constant stress for a prolonged period of time. Three distinct intervals are evident in typical creep (strain vs. time) curves. Primary creep represents the interval in which the structure is changing and is characterized by a decreasing strain rate. During secondary creep, the overall substructure remains essentially constant and a steady-state creep rate is observed. Finally a rapid increase in the strain rate is noted during tertiary creep when the structure beings to break down, ultimately resulting in crack formation and fracture.

Creep is a thermally activated process and is of particular importance at temperatures greater than approximately half of the melting temperature of a material. For plastic deformation occurring as the result of several mechanisms operating simultaneously, the steady-state creep rate may be expressed as:



$$\dot{\varepsilon} = \sum_{i=1} A_i f_i(\sigma,T,S)e^{-Qi/RT} \qquad (1)$$

where $\dot{\varepsilon}$ represents the steady-state creep rate, $A_i$ is a constant, $f_i$ represents the functional dependence for the i'th process, $\sigma$ represents the applied stress, T represents the absolute temperature, Q represents the apparent activation energy for creep, R is the gas constant, and S is a structure parameter which varies with grain size, substructure, and porosity.

Since one mechanism is usually dominant, the steady-state creep rate is often described by an equation of the form

$$\dot{\varepsilon} = A' \sigma^n e^{-Q/RT} \qquad (2)$$

where n is the stress exponent and A' is only approximately constant for any given stress due to a slight dependence on temperature.[14] While Mukherjee et al.[15] have noted that this equation is neither dimensionally or experimentally correct, values for n and Q determined by its use are often presented as evidence that a particular mechanism is the rate-controlling process for creep. Where dislocation processes are likely to dominate creep behavior, it has been reported[15] that the creep rate is more accurately described by an equation of the form

$$\dot{\varepsilon} = A \frac{Gb}{kT} \left(\frac{\sigma}{G}\right)^n D \qquad (3)$$

where G represents the shear modulus, b represents the Burgers vector, D represents the diffusivity, k is the Boltzmann constant, and A and n are dimensionless constants. The diffusivity D can be expressed as $Do^{-Q/RT}$,

where Do is a constant and Q is the activation energy for creep. Good agreement between the apparent activation energy for creep and the activation energy for self-diffusion has been reported for many materials.

A power-law creep relation similar in form to Eq. (3) was considered by Weertman[16] in developing a theory of creep occurring as a result of dislocation climb. Stress exponents between 3 and 4 were predicted. Later it was reported that a stress-exponent of 4.5 could be expected for a dislocation glide and climb process controlled by climb.[17] Nabarro[18] has recently developed a theory of steady-state creep in which dislocation climb takes place without accompanying glide. The stress exponent predicted is 3 or 5 depending on whether dislocations are sources and sinks for vacancies or the rate controlling process is diffusion along dislocation cores. None of these models based on dislocation motion show any grain size dependence.

The effects of vacancy diffusion on high-temperature creep may be significant in many materials under certain conditions. That self-diffusion within the grains of a polycrystalline solid can cause the solid to yield to an applied stress was first noted by Nabarro.[19] A model by which creep deformation might occur as a result of this diffusion was developed by Herring.[20] The creep rate of a material which deforms as a result of the Nabarro-Herring mechanism can be expressed as

$$\dot{\varepsilon} = \alpha \frac{\Omega\sigma}{d^2 kT} D \qquad (4)$$

where $\Omega$ represents the atomic volume, d represents the grain size, and $\alpha$ is a constant approximately equal to 5 in a uniaxial tensile or compressive test. D represents the lattice diffusion coefficient for the



rate-controlling atomic species. For Nabarro-Herring creep the predicted stress-exponent is unity and the creep rate is seen to vary inversely with the square of the grain size.

For diffusion-controlled creep where deformation is the result of diffusion along grain boundaries, Coble[21] has shown that the creep rate varies directly with the first power of stress, as in Nabarro-Herring creep, but inversely with the third power of grain size. The creep rate may be expressed as[22]

$$\dot{\varepsilon} = \simeq 48 \left(\frac{b}{d}\right)^3 \left(\frac{\sigma}{G}\right) Dgb \qquad (5)$$

where Dgb is the diffusion coefficient along grain boundaries.

Since the diffusion coefficients are known to vary exponentially with temperature, and since the creep rates vary inversely with powers of grain size, it is expected that creep by the Nabarro-Herring and Coble mechanisms will be most important at very high temperatures for materials having a small grain size. Nabarro-Herring creep, however, will predominate over high-temperature dislocation-dependent mechanisms only at low stress levels.[22] The activation energy for Nabarro-Herring creep in a pure material is expected to be the same as that for lattice self-diffusion.

Another possible mechanism by which creep occurs in polycrystalline materials is that of grain boundary sliding. While it might be expected that sliding would obey a Newtonian viscosity law, with strain rate proportional to the first power of stress, it has been reported[22] that in cases of macroscopic sliding the stress exponent may have a value of 2 as a result of stress concentrations along the boundaries. Langdon[23] has recently developed a theory of creep deformation by grain boundary

sliding in which sliding occurs by the movement of dislocations along the boundaries by a combination of climb and glide. The strain rate is predicted to be proportional to the second power of stress and inversely proportional to the grain size. These expectations, however, are somewhat different than those predicted by Gifkins,[24] who developed a model of creep in which grain boundary protrusions move along the boundary by diffusion controlled sliding and are accommodated by diffusion around triple points. The predicted stress dependency for deformation occurring in this manner is unity, and the grain size dependency may vary significantly from that determined by Langdon. Since grain boundary sliding ultimately results in cavitation in grain boundaries, followed by fracture, it is expected that the contributions of sliding to creep will be greatest at low stresses and for specimens having a small grain size.

2. Creep in Polycrystalline MgO

The creep of polycrystalline MgO at high temperatures has been extensively investigated under a variety of conditions. As with MgO single crystals, deformation studies have been made in tension, compression, and transverse bending. Vasilos et al.[25] studied the deformation of hot-pressed MgO tested in transverse bending and observed a linear strain rate-stress relation. The measured activation energy for creep at 1200°C was 74 kcal/mole, which is in reasonable agreement with the activation energy for self-diffusion of oxygen in MgO of 62.4 kcal/mole reported by Oishi and Kingery.[26] It was concluded that deformation was the result of Nabarro-Herring or grain boundary diffusion processes. However, in specimens of larger grain size (750μ) evidence of dislocation motion in specimens strained 1-2% at 1500°C was noted.



In a similar but expanded investigation, creep behavior was studied as a function of grain size.[27] It was found that the creep rate was proportional to the first power of stress and $G^{-2.5}$, where G represents the grain size. The activation energy for creep was found to be 54.1 kcal at approximately 1200°C and was independent of grain size in the range 5-20μ. Creep was attributed in part to a stress-directed diffusional mechanism, and discrepancies between observed and calculated creep rates predicted by the Nabarro-Herring equation were related to the observed formation of a dislocation substructure.

Hensler and Cullen[28,29] studied the creep behavior of polycrystalline MgO in compression over a temperature range of 1200-1500°C. For specimens deformed up to 30% no change in grain shape was observed. The stress exponent was determined to be 2.6 ± 0.6, and the measured activation energy for creep was 111 ± 12 kcal/mole. It was reported that no model currently available for creep mechanisms was completely applicable to the results obtained, although deformation was concluded to be the result of extensive grain boundary sliding.

The effects of simultaneous grain growth on the creep of polycrystalline MgO tested in transverse bending has been studied by Tagai and Zisner.[30] An analytical method for separating the growth effect from effects due to creep was devised. While slip lines were observed in deformed specimens, it was estimated that dislocation climb contributed less than 25% to the total creep strain. It was concluded that while creep in polycrystalline MgO is a composite phenomena, deformation occurs primarily by a viscous mechanism of the Nabarro-Herring type. It was determined that the presence of impurities accentuated the diffusion controlled nature of the creep process, presumably by pinning dislocations and inhibiting grain growth.[31]

The creep of polycrystalline MgO tested in compression at 1200°C was recently investigated by Langdon and Pask.[32] The creep rate was found to be independent of grain size, and a stress-exponent of 3.3 was calculated. An activation energy for creep of 51 ± 5 kcal/mole was determined, which is in good agreement with the activation energy for self-diffusion of oxygen in MgO cited previously. It was concluded that the mechanism of dislocation climb was the rate-controlling process for creep of polycrystalline MgO at 1200°C.

C. Deformation in More Complex Systems

In addition to the abundance of information available related to the deformation of single-crystal and polycrystalline MgO, a great many studies have been made of deformation and fracture in practical refractory systems. An understanding of the complex phase relations in these systems is most important before reasonable explanations of mechanical behavior can be made. A number of studies of the complex microstructures typical of practical refractory systems have been reported.[33-35] The growth of individual phases in the presence of a liquid at high temperatures and the effects of composition on the degree of solid-solid bonding have been of prime interest.

Ford et al.[36] measured the strength of chromemagnesite refractories in the temperature range 1290-1575°C. Strength improved as the extent of direct bonding between the magnesite grains and between the chromium-spinel and magnesite grains increased. Baker and Schroth[37] have obtained similar results. The nature of the liquid phase, however, was found by Kriek and Segal[38] to be equally important in determining the high-temperature strength of MgO materials. The lowest strengths were noted for a $CaO/SiO_2$ ratio of 1.0, and the strength reached a maximum when the ratio was equal to 2.0.



The creep of periclase refractory bricks (95-98% MgO) tested in compression over the temperature range 1200-1400°C has been studied by Kreglo and Smothers.[39] The stress exponent varied from 3.8 for a 94.7% MgO brick to 4.5 for a 98.2% MgO brick. The activation energy for the 98.2% MgO brick was determined to be 62 kcal/mole. It was concluded that the predominant mechanism of deformation may be some type of dislocation motion.

Finally, an analysis of the deformation of a firebrick has been made by Hulse and Pask.[40] Experimental results indicated that the flow process is controlled by the amorphous phase in some complex way. The apparent activation energy for creep increased significantly with temperature, possibly due to an increase in liquid content and to the onset of some more complex flow process. It was concluded that a full understanding of the flow process in such materials will require greater study of the interrelationship between character of the materials and the parameters of stress, temperature, and time.

## III. EXPERIMENTAL PROCEDURE

### A. Specimen Preparation

The two-phase system selected for study of mechanical behavior at elevated temperatures consisted of a composition equivalent to varying amounts of $CaO \cdot MgO \cdot SiO_2$ (monticellite) and MgO. The selection of this system as a model was due to the nature of the liquid-solid phase equilibrium at high temperatures and in part also to its specific applicability to practical refractory systems. At temperatures greater than approximately 1500°C the system consists of a liquid silicate phase saturated with MgO. At lower temperatures monticellite crystallizes and two solid phases are present. The possible range of test temperatures is thus similar to that for which polycrystalline MgO has been extensively studied.

Specimens required for mechanical testing were fabricated in several different ways in order to obtain dense materials with varied microstructural characteristics. Reagent grade MgO, $CaCO_3$, and $SiO_2$ were used in the preparation of specimens. Chemical analyses of these powders are listed in the appendix.

Mixtures of MgO, $CaCO_3$, and $SiO_2$ were prepared using amounts of each material calculated to yield final compositions of MgO containing 5%, 10%, and 15% $CaO \cdot MgO \cdot SiO_2$ by weight. The materials were dried in a vacuum oven at 150°C and then dry mixed for 24 hours by tumbling. The mixed powder was placed in a graphite die and cold pressed at 1000 psi. This was followed by vacuum hot pressing. Specimens were heated to 1000°C and held at that temperature for 2 hours to permit $CO_2$ gas formed by the decomposition of $CaCO_3$ to escape. A load of 3000 psi was then applied and maintained constant during continued heating to 1250°C. After pressing at temperature for 30 minutes the load was released and



the specimens cooled to room temperature.

The compacts prepared by hot pressing were heated in air to 1550°C in a quench furnace, held for 2 hours, and rapidly cooled. A number of specimens received an additional 2 hour anneal at 1400°C during cooling. All specimens were stored in a dessicator prior to cutting and testing to minimize surface reactions with moisture in the air. These specimens were designated Type I.

An alternative method of sample preparation for the two-phase materials involved the use of prereacted $CaO \cdot MgO \cdot SiO_2$ powder. A mixture of MgO, $CaCO_3$, and $SiO_2$ calculated to yield a single phase of monticellite upon reaction was prepared by dry mixing. This powder was then placed in a platinum crucible and heated to 1650°C in a gas/air Bickley furnace. Reaction proceeded for 16 hours before the material was cooled to room temperature, crushed to a fine powder (-140 mesh), and examined using optical microscopic techniques and X-ray diffraction. The only crystalline phase which could be detected was $CaO \cdot MgO \cdot SiO_2$; examination of the powder using a polarizing microscope failed to reveal the presence of a glassy phase. The density of the powder was determined to be 3.08 g/cm$^3$ using a helium gas pyncnometer.

A mixture of 85% MgO and 15% $CaO \cdot MgO \cdot SiO_2$ was prepared by dry mixing as before using the prereacted monticellite powder. The hot pressing and sintering steps were identical to those employed in the fabrication of specimens from mixtures containing free $CaCO_3$ and $SiO_2$ with no annealing step on cooling. However, compacts containing approximately 10% and 5% monticellite made with the prereacted $CaO \cdot MgO \cdot SiO_2$ powder were prepared using a technique involving extrusion of a liquid phase at high temperatures as reported by Stoops.[41] Hot pressing a mixture of MgO and 15% $CaO \cdot MgO \cdot SiO_2$ at 1650°C resulted in achieving the

desired composition by controlled extrusion of the liquid phase. Hot pressing the same composition at 1550°C for 30 minutes resulted in only a small loss of liquid. The pressure during hot pressing was maintained at 3000 psi. All specimens formed using the prereacted $CaO \cdot MgO \cdot SiO_2$ were designated Type II.

In order that the mechanical behavior of the $MgO-CaO \cdot MgO \cdot SiO_2$ materials might be compared to the behavior of nominally pure MgO similarly prepared, a number of MgO compacts were made. One set of specimens (Type I) was prepared by hot pressing at 1250°C in vacuum, followed by annealing periods at 1550°C and 1450°C in air similar to those received by Type I specimens containing $CaO \cdot MgO \cdot SiO_2$. A second set of specimens (Type II) was prepared by vacuum hot pressing at 1450°C with no additional treatment.

## B. Specimen Characterization

The density of all specimens was determined using a displacement technique, with mercury as the displacement medium. The density of MgO single crystals as determined by this technique was 3.580 g/cm$^3$. This value was used in the calculation of theoretical densities for the two-phase materials and in the determination of relative densities for the MgO specimens.

All specimens containing $CaO \cdot MgO \cdot SiO_2$ were studied using standard X-ray diffraction techniques. The X-ray diffraction data was of a semi-quantitative nature and was quite useful in comparing $CaO \cdot MgO \cdot SiO_2$ content for different specimens. However, attempts to determine the relative extent of crystallization of $CaO \cdot MgO \cdot SiO_2$ in quenched and annealed specimens using X-ray diffraction data were not successful.

A small section was cut from each specimen and mounted for microscopic examination. Specimens were ground flat using a series of



Buehler emery papers and a diamond wheel. Polishing was completed on a Syntron vibrator with $\alpha-Al_2O_3$ in $H_2O$ or with $\alpha-Al_2O_3$ in a solution of kerosene, glycerine, and $H_2O$ to minimize relief polishing. The specimens of pure MgO were etched for approximately 5 minutes in a 50°C solution of 0.5μ $AlCl_3$ to accentuate grain boundaries. The polished sections were studied using a reflected light microscope, and the microstructural features of each type of specimen were noted. The average grain size of MgO grains for each specimen was determined from photomicrographs using a cross-sectional area technique which took into account the area occupied by the second phase. It was assumed that the volume fraction of the second phase in each material was equal to its fractional area in a polished section.

## C. Mechanical Testing

Specimens for use in mechanical testing were cut from the fired compacts using a diamond blade. All specimens had a length to width ratio of approximately 2:1 and nominal dimensions of 0.600 in. x 0.300 in. x 0.300 in. Specimens were polished using a series of Buehler emery papers and then mounted in a special jig and sanded on both ends to insure that the ends were flat, parallel to each other, and perpendicular to the loading axis.

All mechanical testing was done in compression using the compressive deformation equipment previously described by Hulse and Copley (Apparatus III).[42] High-strength Lucalox $Al_2O_3$ buttons were placed between the specimen and the loading rams, and a thin sheet of platinum foil was placed between the specimen and the $Al_2O_3$ buttons to prevent reaction at high temperatures. Strains were determined during testing by measuring the displacement of two small divot holes located in the side of the $Al_2O_3$ buttons. Pointed sapphire rods were seated in these

divot holes and connected to the pivot arms of the strain-measuring device. The strains were measured using a linear variable differential transformer excited by a Daytronic Differential Transformer Unit. Stresses were measured using similar equipment.

Strain-strain tests were performed on all specimens in the temperature range 1200-1400°C. A Pt/Pt-10% Rh thermocouple located adjacent to the sample was used to measure the temperature during testing. Temperatures were held constant to within ± 1°C of the reported values. A constant loading rate of 55 lb/min. (approximately 600 psi/min. for the specimens used) was employed. Amplified signals from the Daytronic Differential Transformer systems were fed into the channels of a X-Y recorder and a continuous plot of load and engineering strain during the test was obtained. The reported stresses were calculated from the initial cross-section of each specimen. The reported strains are true strains, true strain being defined as the natural logarithm of one plus the engineering strain. All stress-strain tests were carried to fracture since the rate of deformation was generally too high once yielding had occurred to prevent failure.

Creep studies were conducted using the Type II specimen containing approximately 5% $CaO \cdot MgO \cdot SiO_2$. The stress dependency of the creep rate was determined as a function of temperature from 1200-1450°C using an incremental stress technique. The apparent activation energy for creep was determined over the same range of temperatures using the incremental temperature technique described by Dorn.[43] In addition, creep curves obtained at constant stress were measured in the temperature range 1200-1400°C. The stress was maintained constant by increasing the load at intervals of 0.01 engineering strain to compensate for the increase in sample cross-sectional area during the course of a test. The incremental



changes required were calculated assuming constancy of volume and neglecting any barreling that may have occurred. The total strain during creep was measured as in the stress-strain tests and continuously recorded using a recording potentiometer. Overall strain sensitivity was $\pm 5 \times 10^{-4}$. Most specimens were strained approximately 10% before the test was stopped. Good agreement was noted between the recorded strains and the total deformation found by measuring each specimen after testing.

## IV. RESULTS AND DISCUSSION

### A. Specimen Characterization

In the development of materials suitable for study of mechanical behavior at high temperatures, a number of methods of sample fabrication were studied before those methods previously noted were adopted. The principal problems encountered involved the formation of homogeneous structures and the elimination of porosity. The procedure followed for Type I specimens was perhaps the most acceptable method of preparation, although care had to be taken to insure that no $CO_2$ gas remained after hot pressing. The method of liquid extrusion at 1650°C was also an excellent means of sample preparation, but the process was difficult to control and unacceptable at temperatures closer to the incongruent melting point for $CaO \cdot MgO \cdot SiO_2$ of 1492°C.

A number of photomicrographs of polished sections of the specimens used in this study are presented in Figs. 1-4. All specimens containing $CaO \cdot MgO \cdot SiO_2$ were translucent after firing and appeared to be essentially pore free. The absence of detectable porosity is undoubtedly due to the rapid densification rate of materials sintered in the presence of a liquid phase. A theory of liquid phase sintering has been developed by Kingery[44] which can be applied to densification in this system. Densification occurs as a result of a solution-precipitation process due to greater solubility of the solid (MgO) in the liquid (silicate) phase at points of grain contact.

The measured densities of all specimens used for mechanical testing are presented in Table I. The density noted for both Type I and Type II polycrystalline MgO is 99.1% of the value obtained for single crystal MgO. Examination of the photomicrographs of these specimens shown in Fig. 1 reveals the presence of a small amount of porosity within the



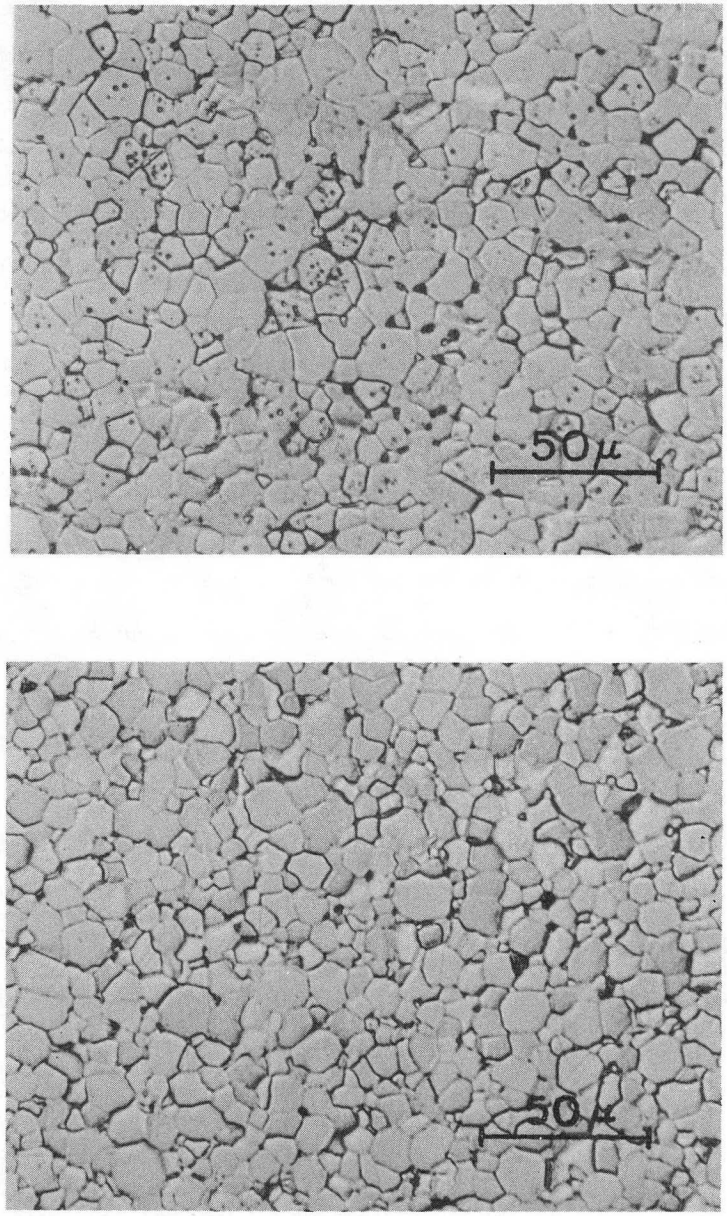


XBB 715-2116

Figure 1. Photomicrographs of polycrystalline MgO specimens, Type I (top) and Type II. $AlCl_3$ etch.

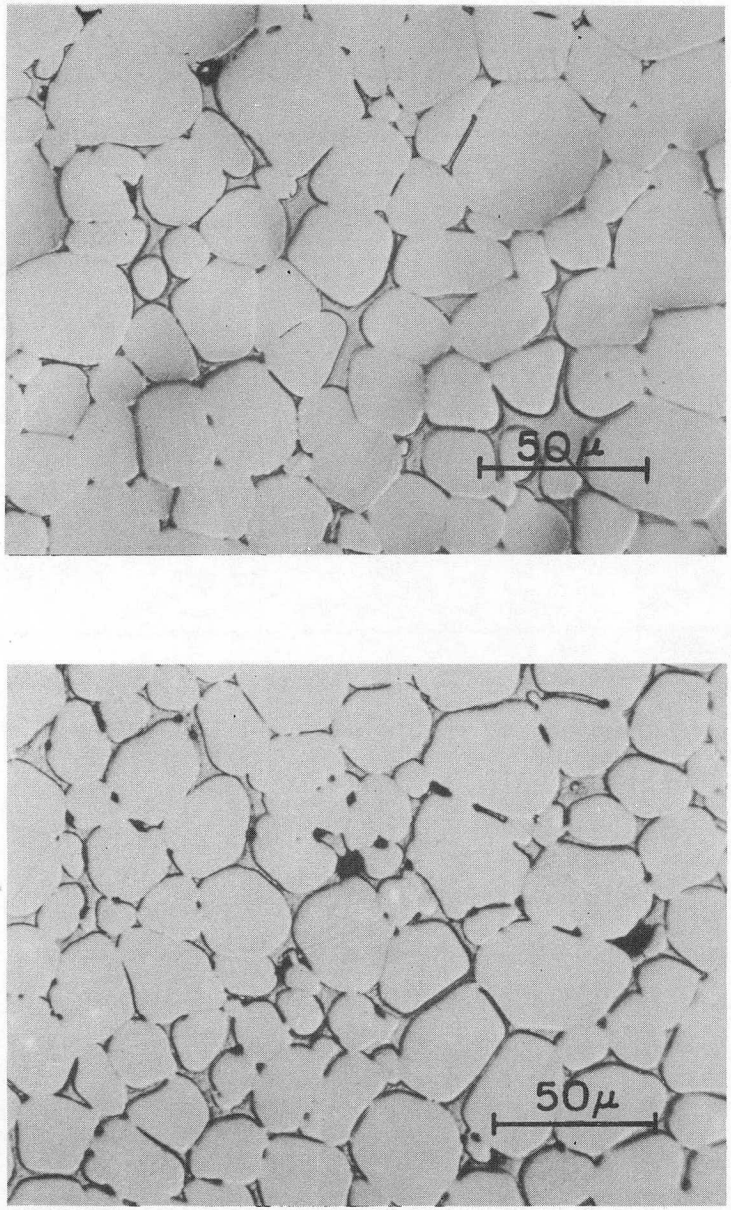


XBB 715-2115

Figure 2. Photomicrographs of specimens containing 5% $CaO \cdot MgO \cdot SiO_2$, Type I (top) and Type II.



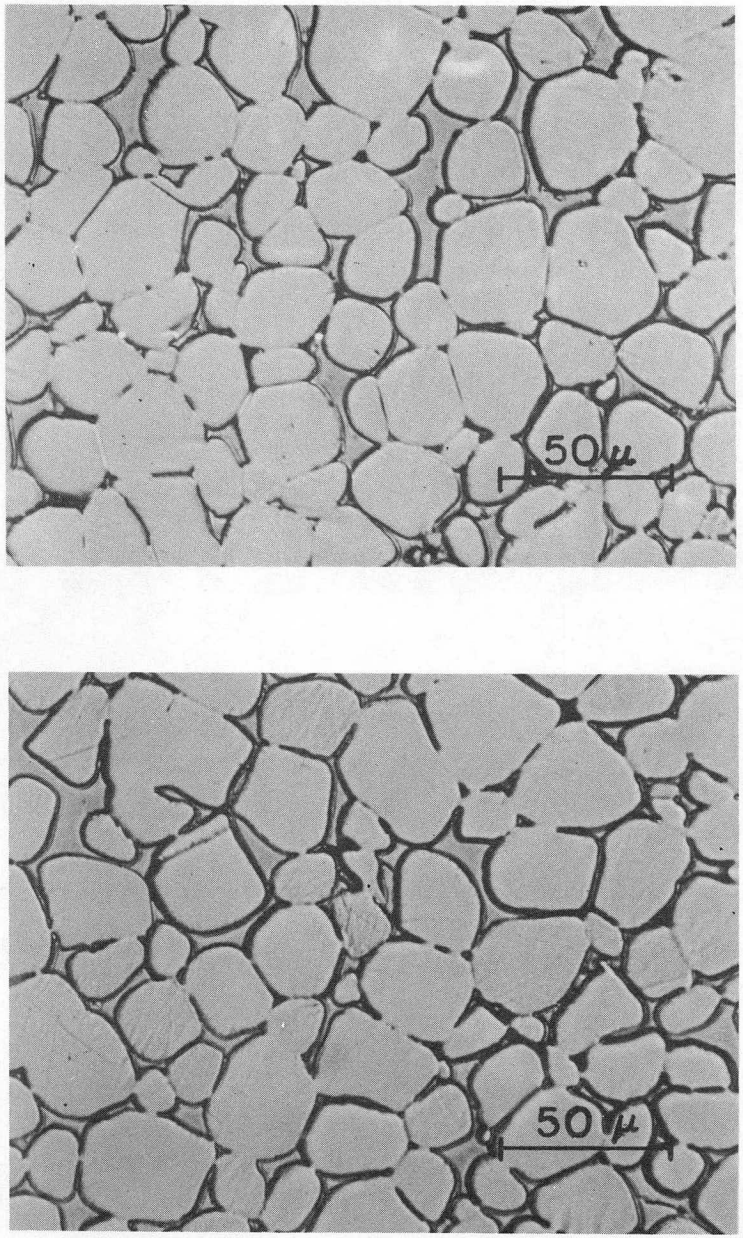


XBB 715-2113

Figure 3. Photomicrographs of Type I specimens containing 10% (top) and 15% $CaO \cdot MgO \cdot SiO_2$.

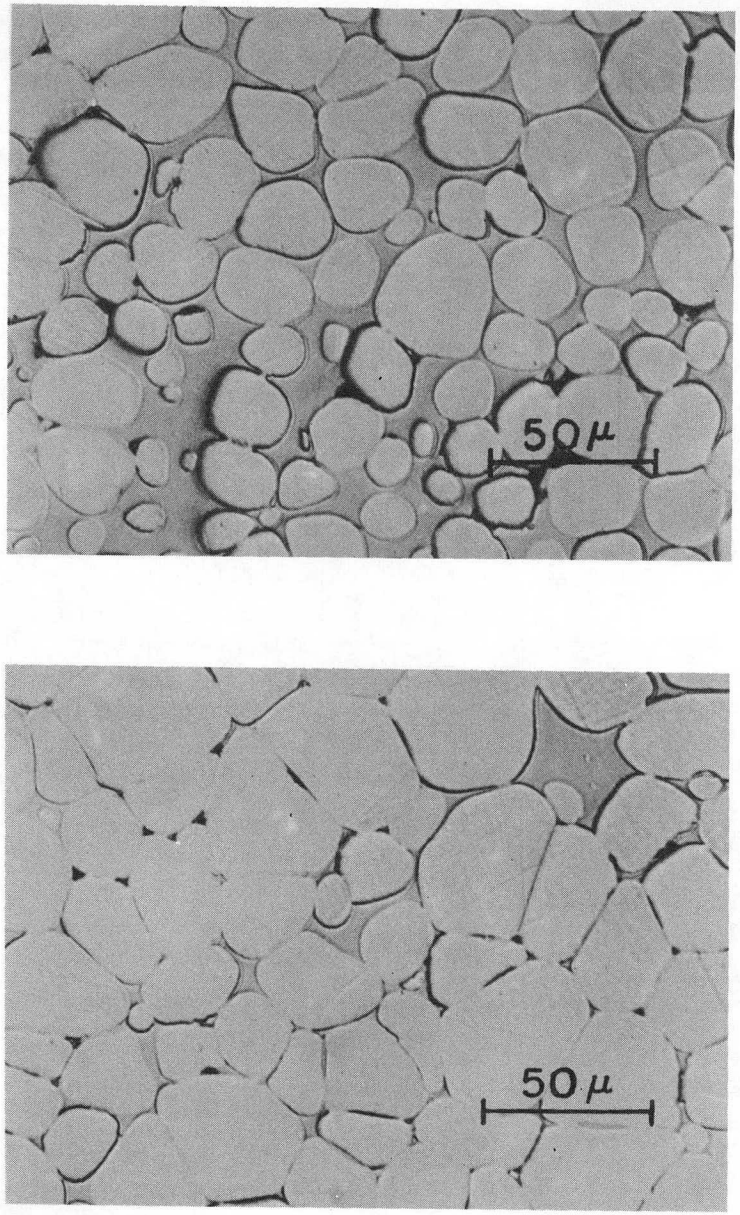


XBB 715-2114

Figure 4. Photomicrographs of the Type II specimen containing 15% $CaO \cdot MgO \cdot SiO_2$.



Table I. Theoretical and measured densities for all specimens studied

| Composition | Density ($g/cm^3$) Type I | Type II | Theoretical |
|---|---|---|---|
| 100% MgO | 3.551 | 3.550 | 3.580 |
| 95% MgO + 5% CMS | 3.498 | 3.496 | 3.552 |
| 90% MgO + 10% CMS | 3.459 | 3.450 | 3.525 |
| 95% MgO + 15% CMS | 3.420 | 3.428 | 3.499 |
| 100% CMS | 3.08 | | 3.05 |

grains of the Type I specimen. The porosity present in the Type II MgO specimen is not so evident and must be concentrated along grain boundaries.

The measured densities presented in Table I for all specimens containing $CaO \cdot MgO \cdot SiO_2$ are seen to be significantly lower than the theoretical values. The theoretical values were calculated assuming a density of 3.08 $g/cm^3$ for $CaO \cdot MgO \cdot SiO_2$ as determined using the powder reacted at 1650°C. While the density of this silicate material is generally reported in the literature as 3.2 $g/cm^3$, calculation of the density from the lattice parameters measured by Sahama and Hytonen,[45] and by Roy,[46] gave a value of 3.05 $g/cm^3$. This value is in good agreement with the value of 3.08 $g/cm^3$ used in the calculation of theoretical densities for the two-phase materials.

For all of the materials containing $CaO \cdot MgO \cdot SiO_2$, the measured densities were approximately 98% of the theoretical values. Since the

specimens were translucent after firing, and since there is no evidence of porosity in the photomicrographs shown in Figs. 2-4, the differences in density noted must be due to the presence of a third undetermined phase. To ascertain what this phase must be, consideration of the phase changes taking place during firing is in order.

Ricker and Osborn[47] have noted that $CaO \cdot MgO \cdot SiO_2$ melts incongruently at 1492°C to give MgO and a liquid phase, together with a small amount of merwinite ($3CaO \cdot MgO \cdot 2SiO_2$) which disappears at approximately 10°C higher. At temperatures up to approximately 1690°C, an equilibrium between MgO and silicate liquid saturated with MgO is established. On cooling, then, merwinite precipitates out of solution at approximately 1502°C and reacts with MgO to form $CaO \cdot MgO \cdot SiO_2$ at 1492°C. The liquid remaining must simultaneously react with MgO to produce additional $CaO \cdot MgO \cdot SiO_2$.

In firing MgO, $CaCO_3$, and $SiO_2$ to form monticellite, the reactions that take place during cooling occur at many sites and the formation of $CaO \cdot MgO \cdot SiO_2$ can proceed rapidly to completion. Thus no second phase was detected in the material reacted at 1650°C and rapidly cooled. However, when a composite material containing $CaO \cdot MgO \cdot SiO_2$ and MgO is heated to temperatures as high as 1550°C or 1650°C, the excess MgO present following melting diffuses through the liquid and deposits onto the surface of neighboring MgO grains. On cooling, the reaction between MgO and merwinite must therefore occur primarily along grain boundaries. The formation of $CaO \cdot MgO \cdot SiO_2$ at these boundaries results in reaction barriers which inhibit complete crystallization of monticellite.

Using standard X-ray diffraction techniques all samples were analyzed to determine the phases present. The only crystalline phases which could be detected were MgO and $CaO \cdot MgO \cdot SiO_2$. It was therefore



concluded that the unknown phase resulting from incomplete reaction on cooling must be of a glassy nature. It was the presence of this glass which resulted in the lower values for density of specimens containing $CaO \cdot MgO \cdot SiO_2$ reported in Table I.

The spatial distribution of a liquid phase relative to solids has been shown by Smith[48] to depend only on the equilibrium dihedral angle. As the equilibrium dihedral angle approaches 0°, the degree of penetration between solid grains by the liquid increases until the liquid extends along all the grain interfaces. Solid grains then exist as islands in a continuous liquid phase. Various aspects of phase distribution in ceramics have been presented by White.[49]

In the system $MgO-CaO \cdot MgO \cdot SiO_2$ an equilibrium dihedral angle of 25° has been reported.[50] Thus, while it is expected that the liquid phase present above 1502°C will penetrate between the solid grains to a considerable degree, a significant amount of MgO grain-grain contacts must remain at equilibrium. Examination of the photomicrographs of materials containing 5-15% $CaO \cdot MgO \cdot SiO_2$ shown in Figs. 2 and 3 indicate that this was precisely the case. However, it is uncertain whether the heat treatments each specimen received were sufficient to establish equilibrium.

The degree of solid-solid (MgO) contact for each specimen was determined using a method described by Stephenson and White.[51] A number of straight lines were drawn on the photomicrographs of each specimen and the number of intersections made by these lines with each of the two types of boundaries was noted. The area of solid-solid interfaces to the total area of all interfaces was then determined as

$$\frac{\text{Area of solid-solid interfaces}}{\text{Total area of all interfaces}} = \frac{N_{ss}}{N_{ss} + N_{sl}}$$

where $N_{ss}$ is the number of intersections with MgO-MgO grain boundaries and $N_{sl}$ is the number of intersections with MgO-CaO•MgO•$SiO_2$ boundaries. The ratios determined are presented in Table II.

Table II. Average grain size and degree of MgO grain-grain contact for the specimens studied

| Composition | Average Grain Size | | $\frac{N_{ss}}{N_{ss} + N_{sl}}$ | |
|---|---|---|---|---|
| | Type I | Type II | Type I | Type II |
| 100% MgO | 17.0μ | 12.8μ | 1.0 | 1.0 |
| 95% MgO + 5% CMS | 29.6μ | 31.3μ | 0.51 | 0.28 |
| 90% MgO + 10% CMS | 25.2μ | - | 0.37 | - |
| 85% MgO + 15% CMS | 22.1μ | - | 0.26 | - |

For the Type I specimens shown in Fig. 2 (top) and Fig. 3, it is evident that as the amount of CaO•MgO•$SiO_2$ is increased, the degree of solid-solid contact decreases. For 5% CaO•MgO•$SiO_2$ the ratios of solid-solid (MgO) area to the total area of the boundaries was 0.51, while the ratio decreased to 0.26 for specimens containing 15% of the second phase. For the Type II specimens the distribution of the second phase after firing was relatively uniform only for the specimen containing 5% CaO•MgO•$SiO_2$. This specimen was formed by extrusion of the liquid phase at 1650°C and the CaO•MgO•$SiO_2$ content was estimated to be 5% based on the density measurement, X-ray diffraction data, and examination of microstructure. The ratio of solid-solid interfacial area to the total interfacial area for this specimen was found to be 0.28, or approximately the same as that for the Type I specimen containing 15% CaO•MgO•$SiO_2$.



For the Type II specimens containing 10% and 15% CaO•MgO•$SiO_2$ the distribution of the monticellite phase was very non-homogeneous. As shown in Fig. 4, the CaO•MgO•$SiO_2$ content was very high in some areas while in other areas the content was very low. This effect was the result of poor mixing of the prereacted CaO•MgO•$SiO_2$ powder with the MgO during the initial stages of fabrication. Extrusion of the liquid phase at 1550°C, as for the sample containing 10% monticellite, or hot pressing at 1250°C followed by sintering at 1550°C, as for the 15% specimen, did not permit redistribution of the liquid as was obtained in the specimen pressed at 1650°C where the liquid was less viscous. From Fig. 4 it is also apparent that equilibrium was not established between the solid and liquid phases since the solid grains are completely surrounded by CaO•MgO•$SiO_2$ in the regions of high concentration. Due to the non-homogeneity of the Type II specimens containing 10% and 15% CaO•MgO•$SiO_2$, it was not possible to obtain a meaningful figure for the ratio of solid-solid interfacial area to the total interfacial area.

The effects of the CaO•MgO•$SiO_2$ phase on grain growth of MgO grains have been noted for the various specimens. The average grain size for each specimen is included in Table II. In the absence of CaO•MgO•$SiO_2$, the average grain sizes for the Type I and Type II MgO specimens were 17.0μ and 12.8μ respectively. As the CaO•MgO•$SiO_2$ content was increased from 5-15% in the Type I specimens, the grain size decreased from 29.6μ to 22.1μ. Since grain growth in the presence of the liquid is a solution diffusion-precipitation process,[52] any increase in the diffusional path must result in a decrease in the growth rate. The effects of grain growth retardation in the presence of the liquid phase is most evident in Fig. 4, where the grain size in the region of high CaO•MgO•$SiO_2$ concentration is seen to be much smaller than in the region of low

concentration. Similar results of the inhibiting effect of the liquid on MgO grain growth in this system have been reported by Buist et al.[52]

B. Stress-Strain Tests

The stress-strain curves obtained for polycrystalline MgO and for MgO-CaO•MgO•$SiO_2$ materials are presented in Fig. 5 and Figs. 8-10 for the various test temperatures. Type I and Type II specimens of similar composition are presented in a single figure to facilitate comparison of the behavior of the two types of materials. In addition, the curves have been replotted in Figs. 11-16 as a function of composition at each test temperature. The offset yield stress, the maximum stress before fracture, and the strain at fracture for each specimen of Type I and Type II are given in Tables III and IV, respectively.

1. Polycrystalline MgO

The significance of the character of grain boundaries in influencing deformation of polycrystalline MgO becomes evident upon examination of Fig. 5. The stress-strain behavior exhibited by the two types of MgO in the temperature range 1200-1400°C is seen to be markedly different. The Type II specimens have a fracture stress much greater than the Type I specimens, but the Type I specimens exhibit much more ductility before fracture. At 1200°C, for example, fracture in the Type I specimen occurred only after it had been deformed approximately 13%, and the maximum stress was 23,850 psi. The Type II specimen tested at 1200°C was able to deform less than 1% before it fractured at a stress level of 29,600 psi. Similar comparisons were noted for specimens tested at 1300°C and 1400°C.

For the Type I specimens of MgO, which were hot pressed and then annealed at 1550°C, it was observed that the porosity present was primarily within the grains. For the Type II specimens, which were not



Table III. Stress-strain data for specimens of Type I

| Composition | Yield Stress | Fracture Stress | Strain at Fracture |
|---|---|---|---|
| (1) 100% MgO | | | |
| 1200°C | 10,400 psi | 23,850 psi | 13.2% |
| 1300°C | 8,100 psi | 16,400 psi | 13.0% |
| 1400°C | 7,800 psi | 12,500 psi | >8.0% |
| (2) 5% CaO•MgO•$SiO_2$ | | | |
| 1200°C | 11,300 psi | 13,640 psi | 2.32% |
| 1300°C | 5,800 psi | 7,500 psi | 2.40% |
| 1400°C | 4,000 psi | 6,630 psi | 2.20% |
| (3) 10% CaO•MgO•$SiO_2$ | | | |
| 1200°C | 14,000 psi | 17,580 psi | 2.68% |
| 1300°C | 7,900 psi | 10,000 psi | 2.30% |
| 1400°C | 4,500 psi | 6,870 psi | 2.20% |
| (4) 15% CaO•MgO•$SiO_2$ | | | |
| 1200°C | 16,400 psi | 22,400 psi | 5.20% |
| 1300°C | 12,400 psi | 16,500 psi | 4.20% |
| 1400°C | 8,000 psi | 10,100 psi | 3.10% |

Table IV. Stress-strain data for specimens of Type II

| Composition | Yield Stress | Fracture Stress | Strain at Fracture |
|---|---|---|---|
| (1) 100% MgO | | | |
| 1200°C | 29,000 psi | 29,600 psi | 0.97% |
| 1300°C | 20,000 psi | 27,000 psi | 1.76% |
| 1400°C | 15,200 psi | 24,500 psi | 4.90% |
| (2) 5% $CaO \cdot MgO \cdot SiO_2$ | | | |
| 1200°C | 15,500 psi | 22,840 psi | 2.50% |
| 1300°C | 11,400 psi | 18,560 psi | 4.18% |
| 1400°C | 7,600 psi | 10,580 psi | 2.78% |
| (3) 10% $CaO \cdot MgO \cdot SiO_2$ | | | |
| 1200°C | 14,600 psi | 19,100 psi | 2.73% |
| 1300°C | 7,000 psi | 10,400 psi | 2.32% |
| 1400°C | 5,800 psi | 7,270 psi | 2.22% |
| (4) 15% $CaO \cdot MgO \cdot SiO_2$ | | | |
| 1200°C | 10,500 psi | 12,840 psi | 2.22% |
| 1300°C | 6,200 psi | 8,140 psi | 2.32% |
| 1400°C | 6,000 psi | 7,080 psi | 2.30% |



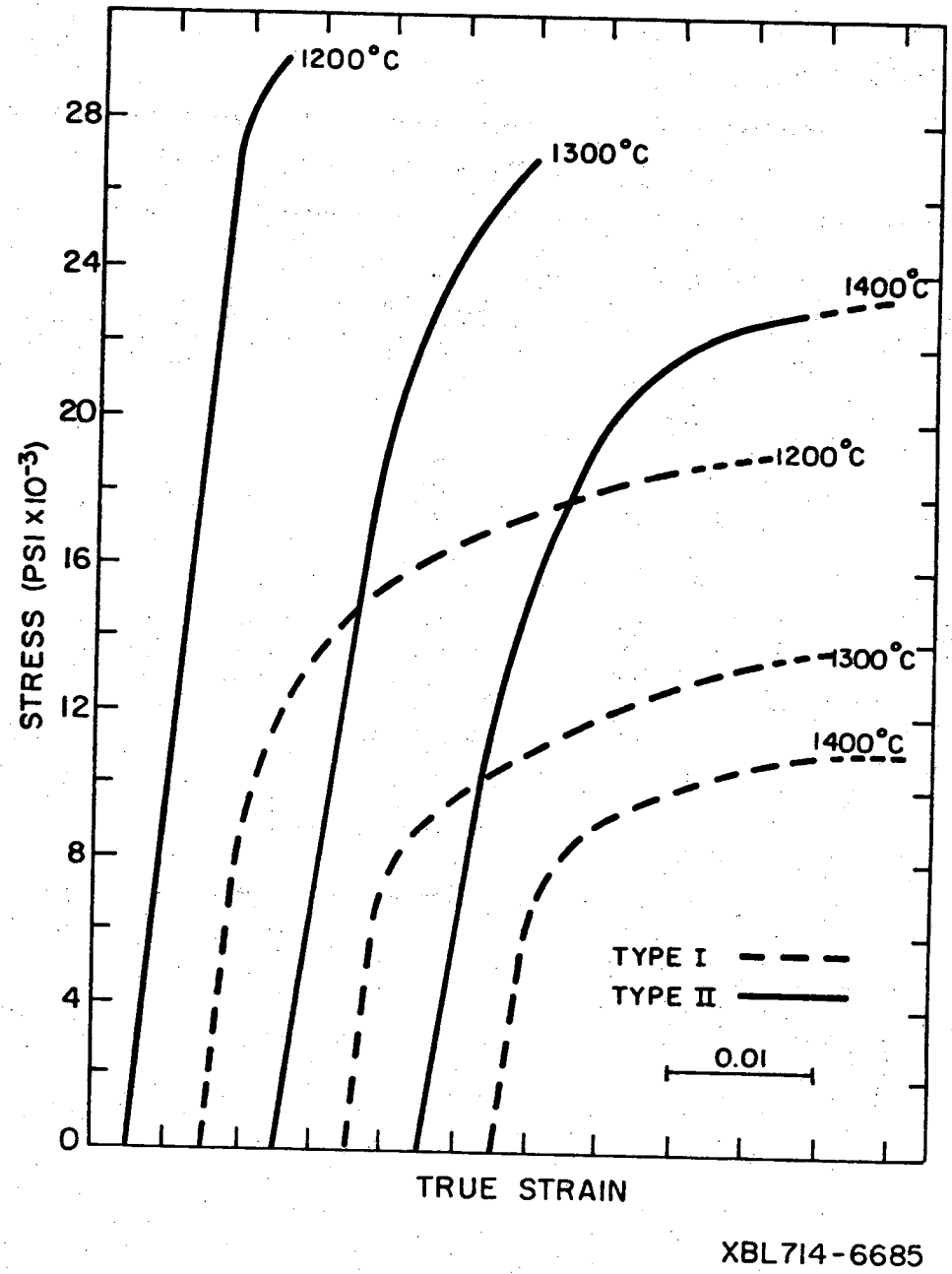


Figure 5. Stress-strain curves for the specimens of polycrystalline MgO.

annealed, pores were present primarily along the boundaries. It has been shown that the presence of porosity along grain boundaries in MgO inhibits dislocation motion and leads to separation of grain boundaries.[12b] Fracture in specimens of this type is then essentially brittle, occurring when the level of stress is sufficiently high to propagate an existing flaw to failure. Figure 6 is a scanning electron micrograph of the fracture surface of a Type II MgO specimen deformed approximately 1% at 1200°C. The fracture path is seen to be completely intergranular, as expected from examination of the corresponding stress-strain curve in Fig. 5. While the total strain at fracture for Type II specimens tested at 1300°C and 1400°C was greater than that at 1200°C, the fracture path was intergranular in all cases.

The ductility exhibited by Type I specimens of MgO can be attributed to the stronger grain boundaries characteristic of these specimens. Since the integrity of the grain boundaries is maintained during loading, the development of stress concentrations and the initiation of slip on a number of slip systems results in yielding of the material at lower stress levels than for Type II specimens. The yield stress at 1200°C for the Type II specimen, for example, was 29,000 psi, approximately equal to the stress at fracture. The yield stress of the Type I specimen at the same temperature was 10,400 psi, or less than half of the stress at fracture. The behavior of Type I specimens during loading has been described by Copley and Pask.[12a] As the applied stress is increased slip occurs first on the $\{110\}\langle 1\bar{1}0\rangle$ slip systems due to their lower resistance to dislocation motion. Long range stresses build up in each grain and soon force slip on the $\{001\}\langle 1\bar{1}0\rangle$ slip systems. Since five independent slip systems are then in operation, yielding occurs in the polycrystalline material.



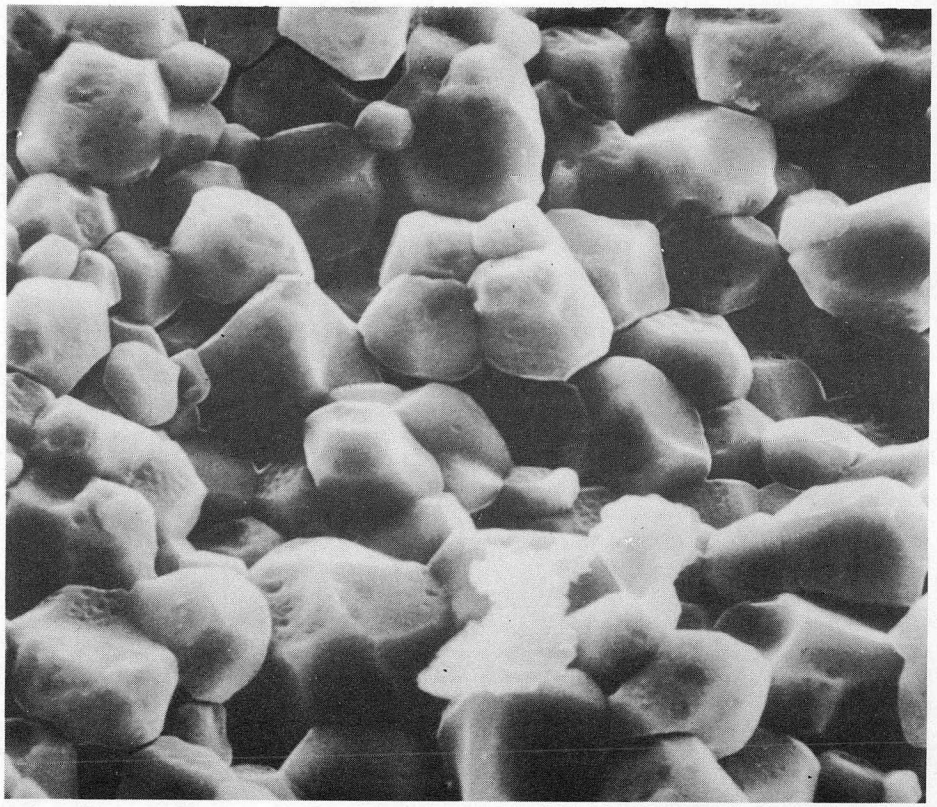

XBB 715-2110

Figure 6. Scanning electron micrograph of the fracture surface of a Type II specimen of MgO strained ~1% at 1200°C. Intergranular fracture. 2000X

For specimens deforming as the result of extensive dislocation motion, work hardening generally occurs as dislocations become entangled. Thus the increase in the strain rate after yielding is very gradual and the stress level at fracture may be much greater than the stress level required for yielding. In a stress-strain experiment the slope of the stress-strain curve is related to the strain rate by the equation

$$\frac{d\sigma}{d\varepsilon} = \left(\frac{d\sigma}{dt}\right)\left(\frac{d\varepsilon}{dt}\right)^{-1} \qquad (6)$$

where $\sigma$ represents the applied stress, $\varepsilon$ represents the strain, and t represents time. For a constant loading rate, a high slope indicates a low strain rate, and a low slope indicates a high strain rate. In Fig. 5 the effects of work hardening in the Type I specimens are reflected in the increase in stress required following yielding to cause further increases in strain.

Since deformation in Type I specimens of MgO occurs as a result of extensive dislocation motion, it is expected that fracture will eventually occur across the grains. Examination of the fracture surface shown in Fig. 7 of a Type I specimen of MgO deformed approximately 13% at 1200°C reveals extensive grain deformation and indicates transgranular fracture. Similar observations have been made by a number of investigators, including Copley and Pask,[12a] and Vasilos et al.[10] for materials possessing strong grain boundaries.

2. <u>MgO-CaO•MgO•$SiO_2$ Specimens</u>

The stress-strain relations for materials containing 5-15% CaO•MgO•$SiO_2$ and MgO in the temperature range 1200-1400°C are presented in Figs. 8-10. For smaller amounts of CaO•MgO•$SiO_2$ (Figs. 8 and 9) the Type II specimens were significantly stronger than the Type I specimens,



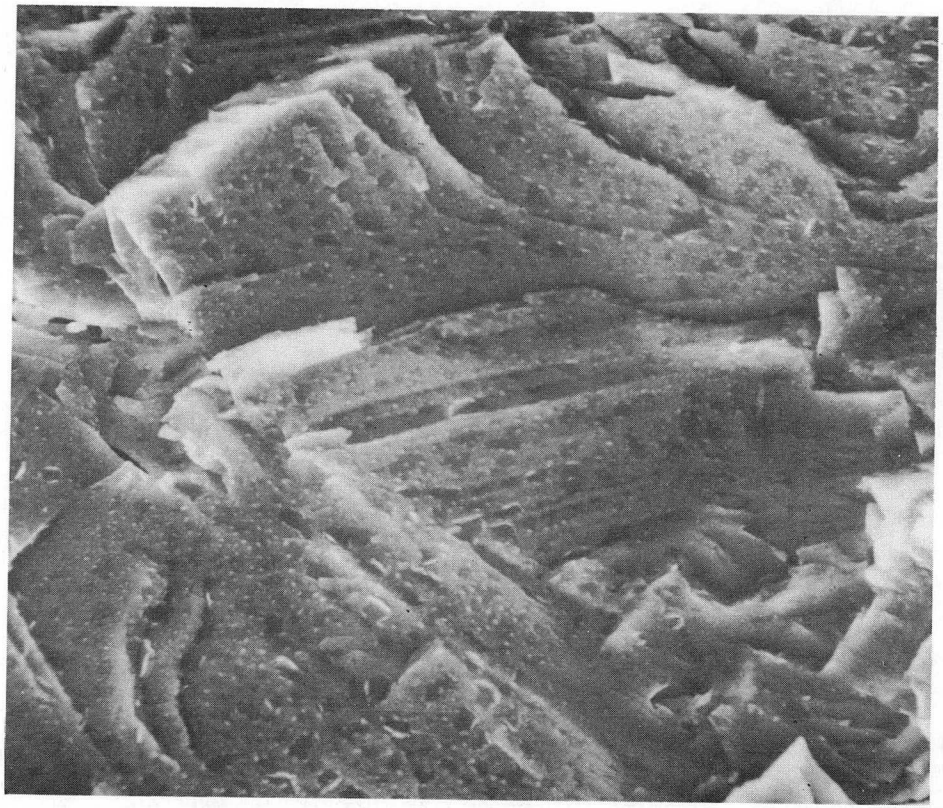

XBB 715-2111

Figure 7. Scanning electron micrograph of the fracture surface of a Type I specimen of MgO strained ~13% at 1200°C. Transgranular fracture. 2000X

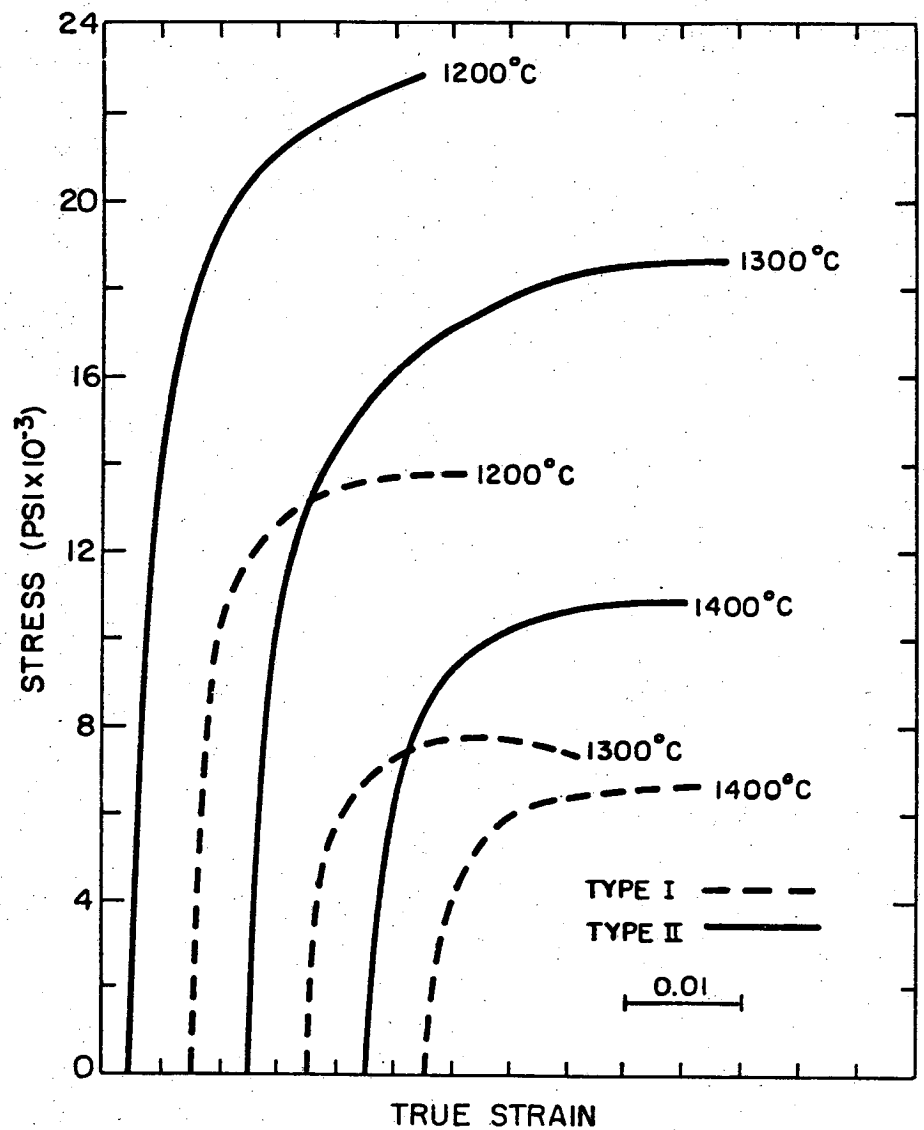


XBL714-6682

Figure 8. Stress-strain curves for specimens containing 5% $CaO \cdot MgO \cdot SiO_2$.



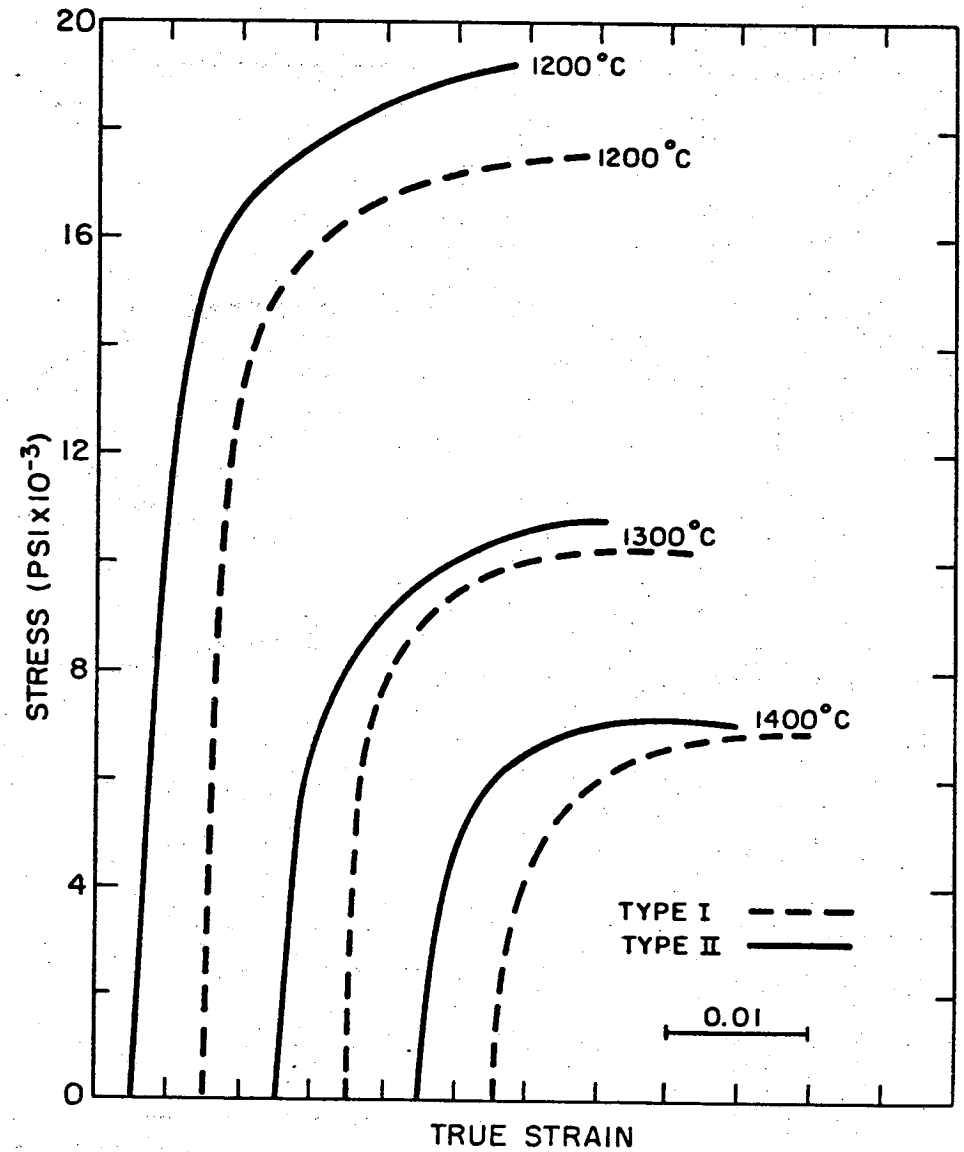


XBL714-6683

Figure 9. Stress-strain curves for specimens containing 10% $CaO \cdot MgO \cdot SiO_2$

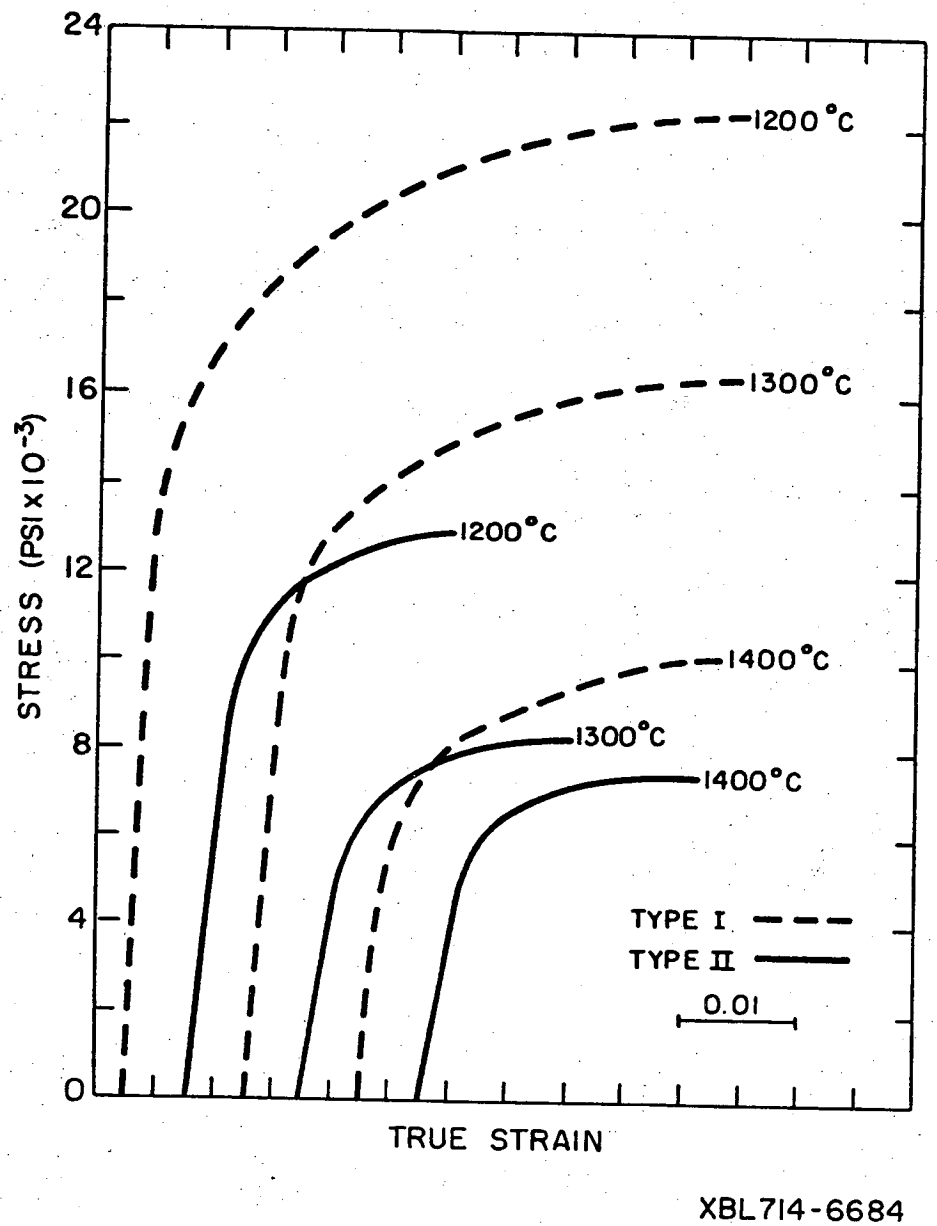


Figure 10. Stress-strain curves for specimens containing 15% $CaO \cdot MgO \cdot SiO_2$.



although the general shape of the curves was quite similar. For specimens containing 15% $CaO \cdot MgO \cdot SiO_2$, however, it is evident from Fig. 10 that the Type I specimens have greater strength over the range of temperatures used in this study.

The differences in mechanical behavior of Type I and Type II specimens containing $CaO \cdot MgO \cdot SiO_2$ become more apparent upon examination of Figs. 11-16. For the temperatures noted, the strength of Type I specimens (Figs. 11-13) was observed to increase as the amount of second phase present was increased. However, the fracture stresses for the specimens containing 5% and 10% $CaO \cdot MgO \cdot SiO_2$ were considerably lower than for Type I specimens of MgO at corresponding temperatures. For the 15% specimens of Type I, the fracture stresses were approximately equal to those for the pure MgO specimens at the corresponding temperatures. The behavior of Type II specimens (Figs. 14-16) containing $CaO \cdot MgO \cdot SiO_2$ was somewhat different than that of Type I specimens. As the amount of $CaO \cdot MgO \cdot SiO_2$ was increased, the strength of all Type II specimens was observed to decrease. The fracture strengths determined for all Type II specimens containing $CaO \cdot MgO \cdot SiO_2$ were significantly lower than those for MgO specimens of Type II at the same temperatures. However, it may be more realistic to compare these fracture stresses with those of the Type I specimens of MgO since the firing temperatures for Type II specimens containing $CaO \cdot MgO \cdot SiO_2$ were higher than for the pure MgO specimens of the same type. For this comparison, it was noted that the 5% $CaO \cdot MgO \cdot SiO_2$ specimens have fracture strengths approximately equaling those of pure MgO in the temperature range 1200-1400°C.

It was hypothesized that the differences in behavior observed for the two types of specimens containing $CaO \cdot MgO \cdot SiO_2$ might be due to variations in the amount of the silicate phase remaining uncrystallized

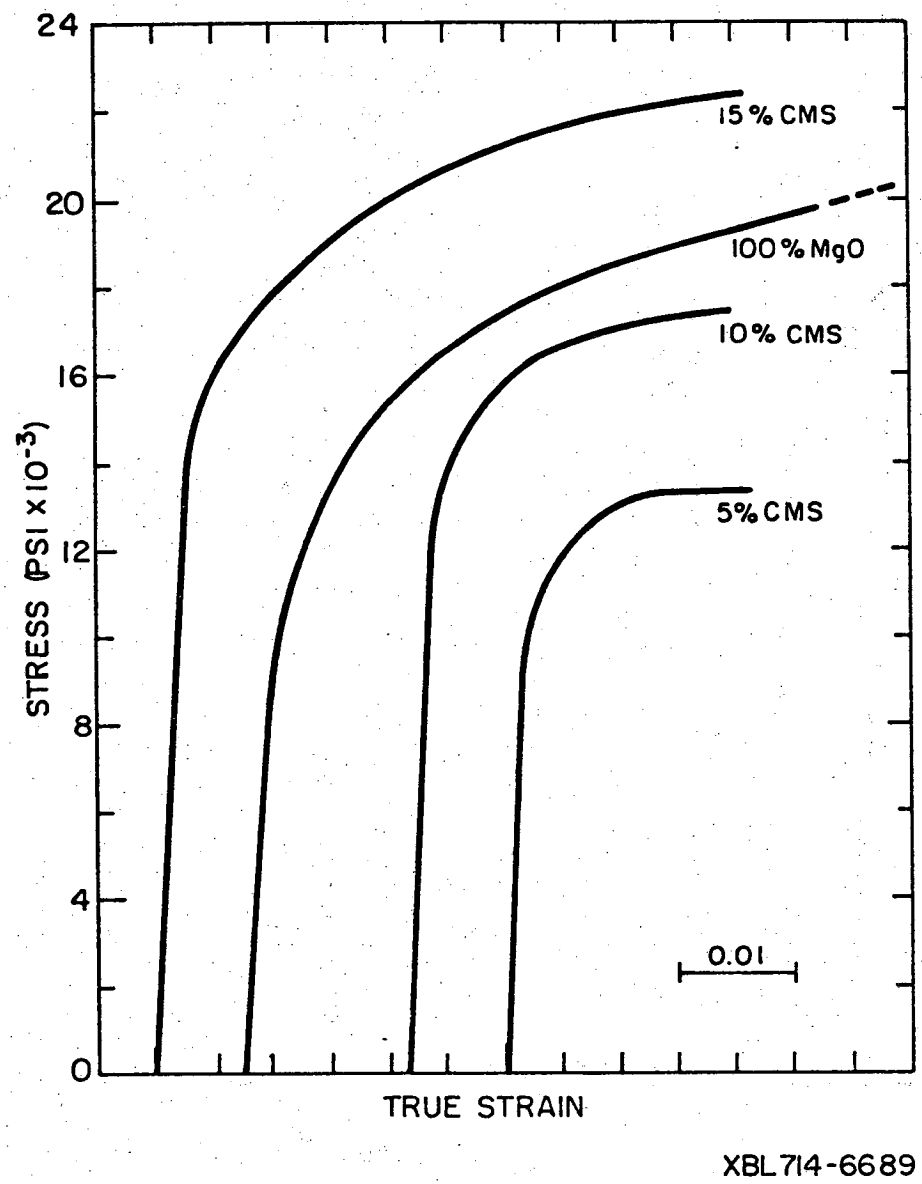


Figure 11. Stress-strain curves for Type I specimens tested at 1200°C.



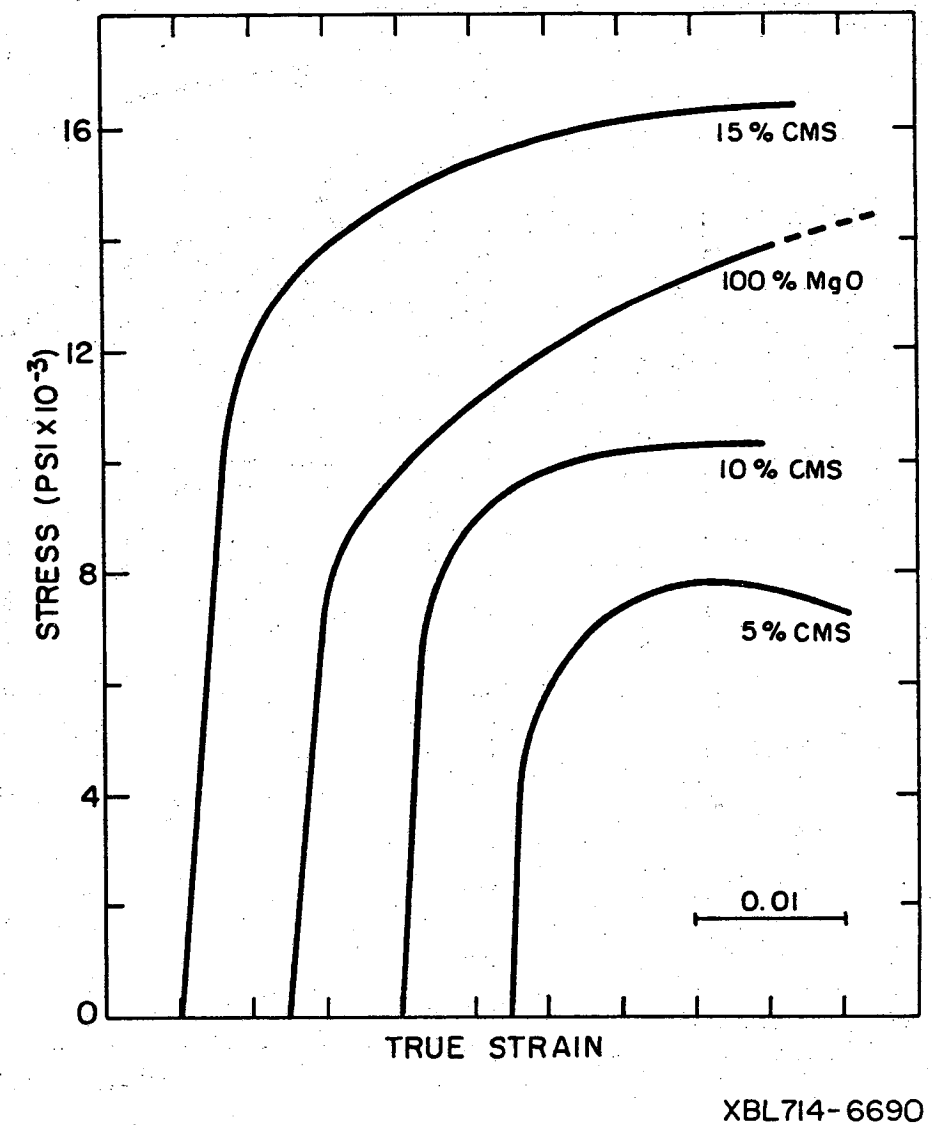


Figure 12. Stress-strain curves for Type I specimens tested at 1300°C.

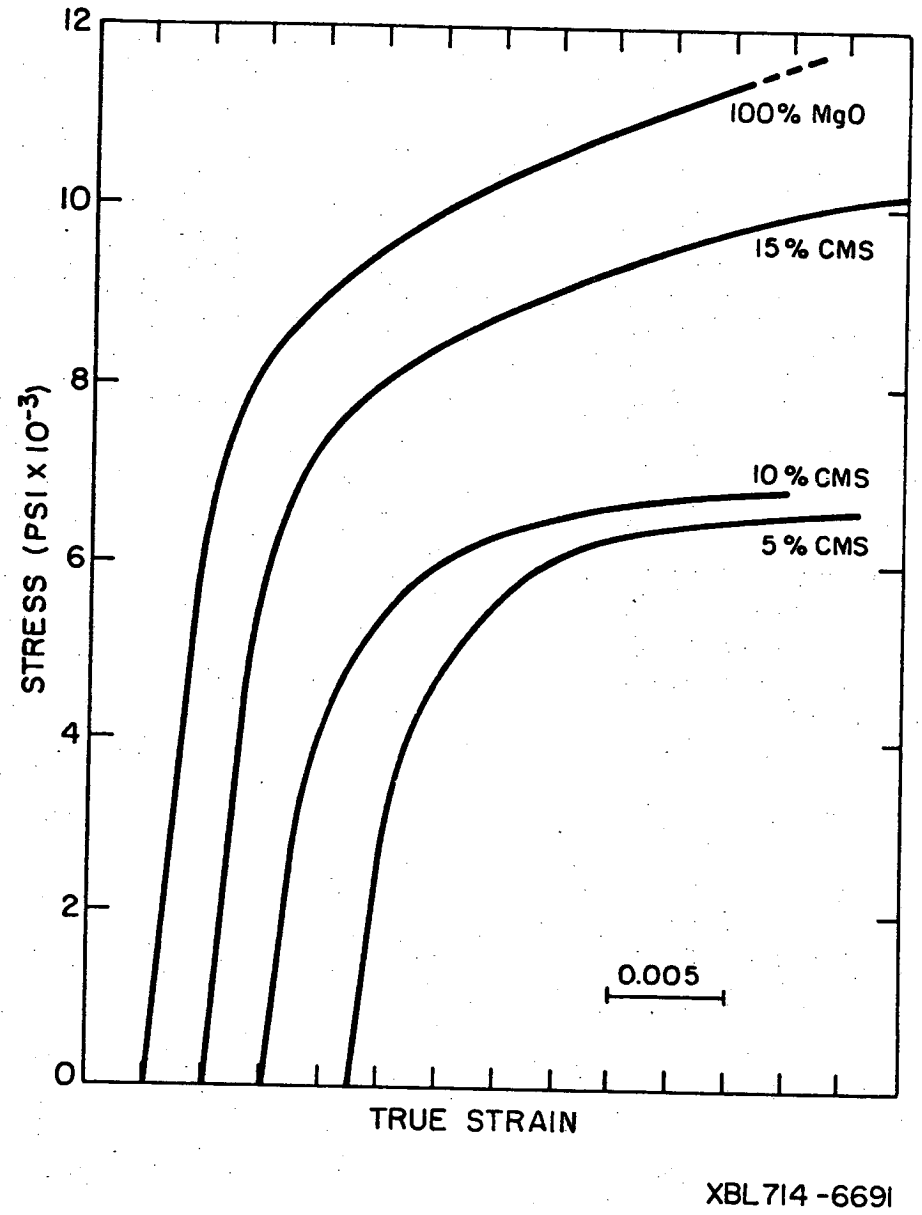


Figure 13. Stress-strain curves for Type I specimens tested at 1400°C.



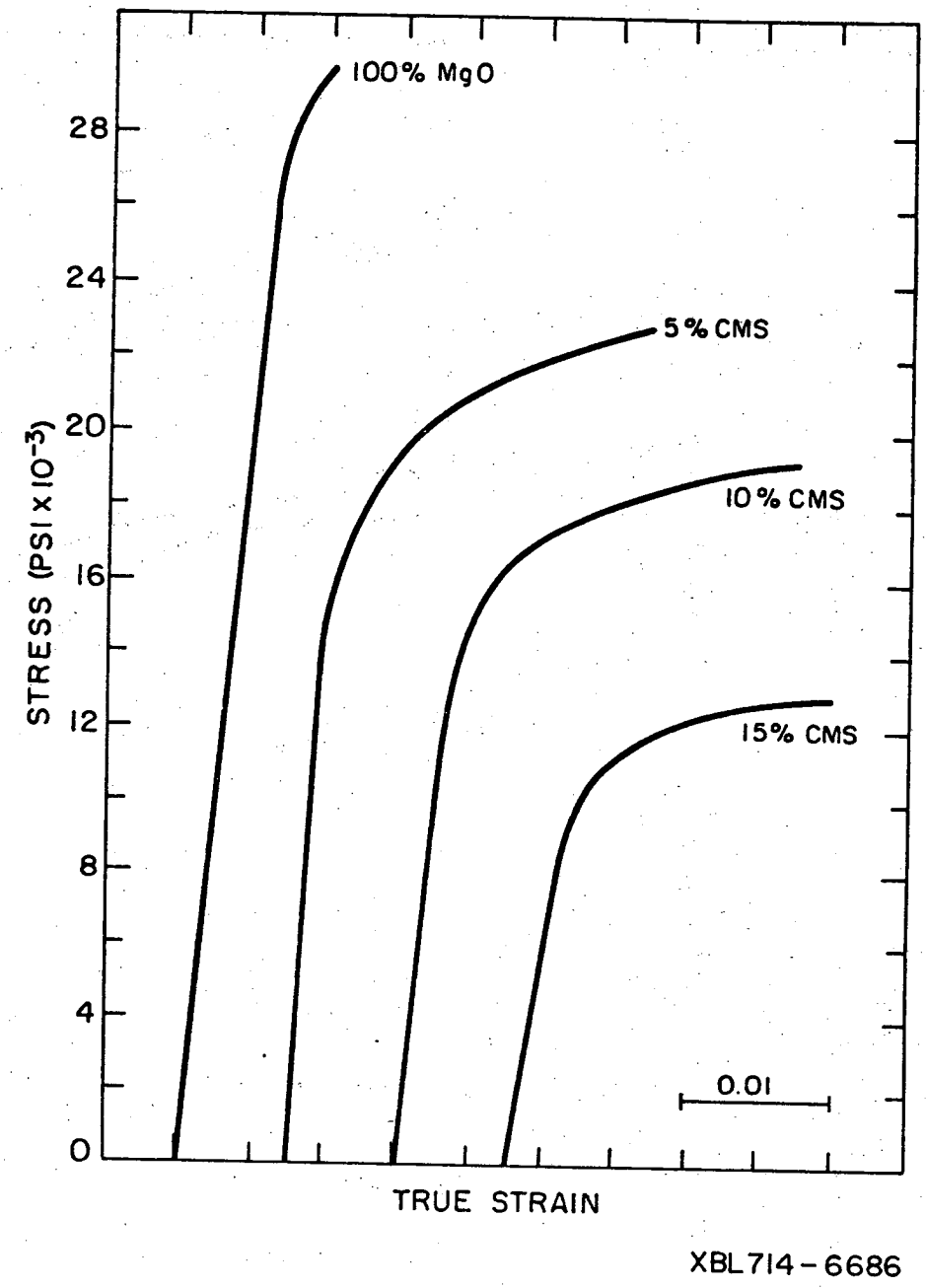


igure 14. Stress-strain curves for Type II specimens tested at 1200°C.

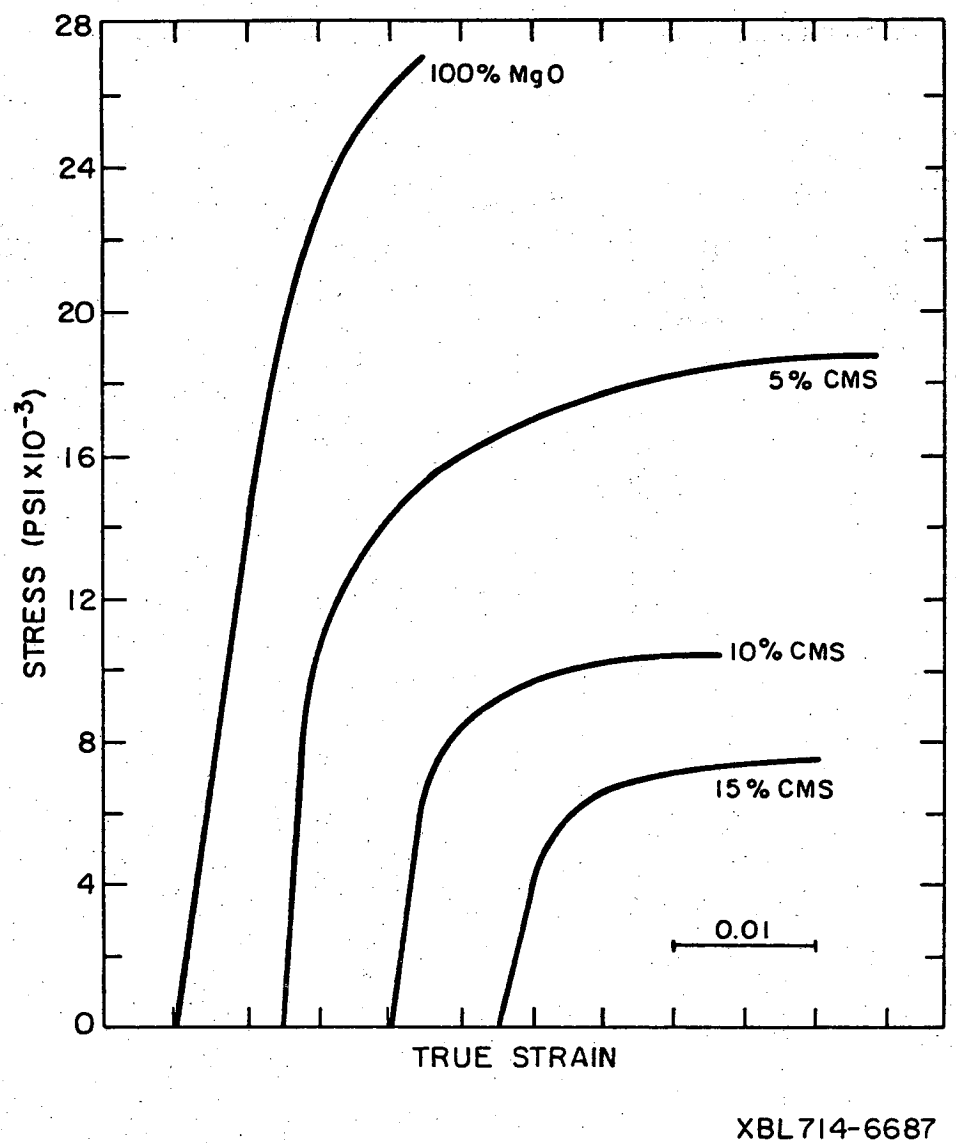


Figure 15. Stress-strain curves for Type II specimens tested at 1300°C.



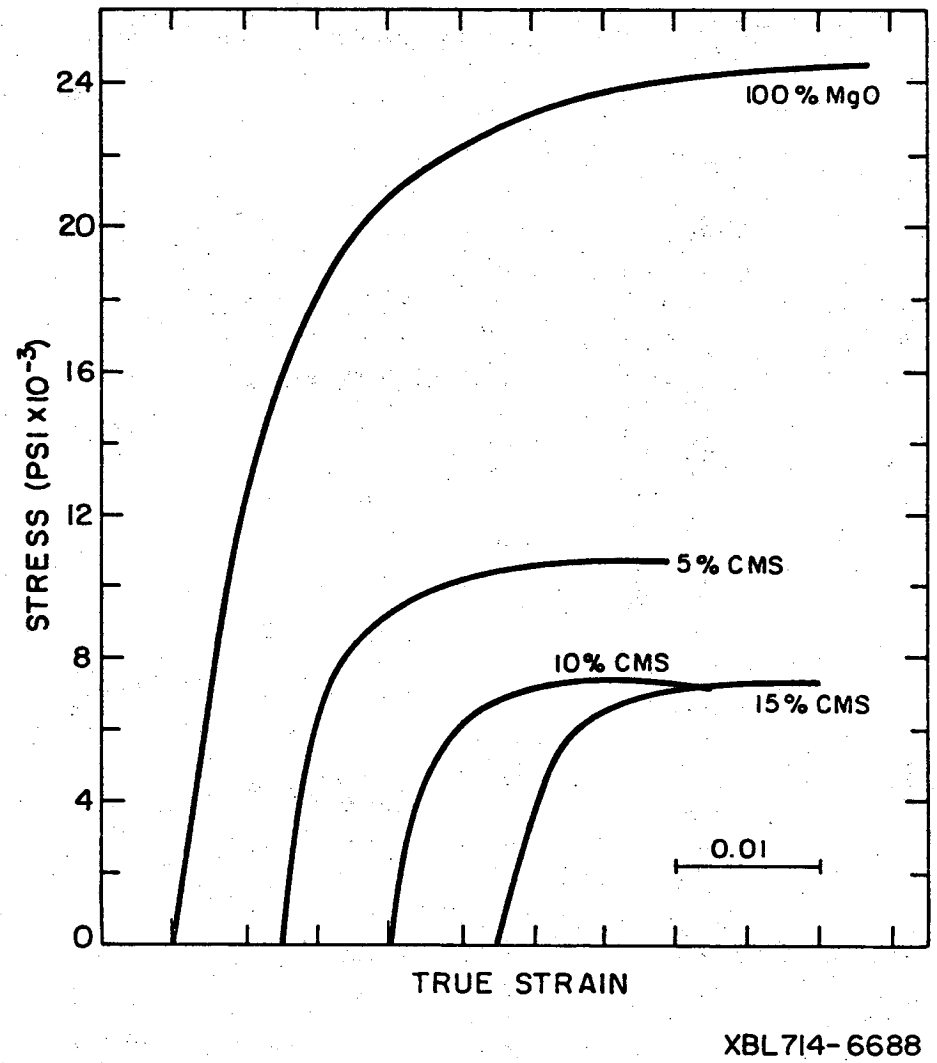


Figure 16. Stress-strain curves for Type II specimens tested at 1400°C.

after firing. Accordingly, a number of attempts were made to alter the glassy content of these materials. Analysis of specimens quenched from 1550°C using density measurements and standard X-ray diffraction techniques failed to reveal any significant differences from specimens annealed at 1400°C for up to 40 hours. Therefore the reactions to form $CaO \cdot MgO \cdot SiO_2$ upon cooling were shown to occur rapidly, and the reaction barriers which prevent complete crystallization of $CaO \cdot MgO \cdot SiO_2$ from the liquid must exist as previously proposed. Furthermore, the differences in behavior for Type I and Type II specimens must arise from effects of $CaO \cdot MgO \cdot SiO_2$ distribution, and the corresponding effects on the continuity of the MgO structure.

While the fracture stresses for Type I materials containing 5% and 10% $CaO \cdot MgO \cdot SiO_2$, and for Type II materials containing 10% and 15%, were significantly lower than for the Type I specimens of pure MgO, it is interesting to note that at 1200°C the yield stresses for all the specimens containing $CaO \cdot MgO \cdot SiO_2$ were higher than the corresponding yield stresses in the Type I specimens of MgO. Since yielding in the MgO specimens is dependent upon dislocation motion, the presence of $CaO \cdot MgO \cdot SiO_2$ along grain boundaries must restrict that motion and thereby increase the stress required for yielding. As the distribution of $CaO \cdot MgO \cdot SiO_2$ is made more uniform, the inhibiting effect on slip must become more pronounced.

The values presented in Table II for the ratio of solid-solid interfacial area to the total interfacial area for various specimens may be considered to be a measure of the degree of uniformity of distribution of the silicate phase in the system being studied. As the ratio decreases, the uniformity of distribution of the silicate phase increases. This is evident upon examination of the photomicrographs in



Figs. 2-4. For the Type II specimens containing 15% $CaO \cdot MgO \cdot SiO_2$ it was impossible to determine the area ratio due to gross variations in silicate phase distribution. The yield stress for this specimen at 1200°C was only slightly greater than that of the Type I MgO specimens at the same temperature. For the 5% specimen of Type II, which had an area ratio of 0.28 and the most uniform distribution of $CaO \cdot MgO \cdot SiO_2$, the increase in yield stress compared to that for pure MgO was approximately 50%. Similar increases in yield stress can be cited for Type I specimens. In the 5% specimen of Type I which had an area ratio of 0.51, the presence of $CaO \cdot MgO \cdot SiO_2$ increased the yield stress approximately 10%. The 15% specimen of Type I, which had an area ratio of 0.26 and was similar in appearance to the 5% specimen of Type II, had a yield stress approximately 57% greater than that for the Type I specimen of MgO.

The effect of silicate phase distribution on the yield stress was not so evident at temperatures of 1300°C and 1400°C. For the two specimens having the most uniform distribution of the silicate phase (Type I - 15%, Type II - 5%), the yield stress continued to be greater than for the MgO specimens of Type I. For all other specimens containing $CaO \cdot MgO \cdot SiO_2$ the yield stresses were lower than those determined for MgO specimens of Type I at corresponding temperatures. It is likely that this observed decrease is due to yielding of the silicate phase following continued softening of the residual glass at higher temperatures. As the uniformity of distribution of the silicate phase increases, yielding can occur more uniformly throughout the specimen. Consequently, the Type I specimens containing 5% and 10% $CaO \cdot MgO \cdot SiO_2$ yield at lower stresses than do the non-homogeneous specimens of Type II for temperatures where deformation of the silicate phase is important.

It remains unclear why this effect should not be equally important in the specimens having greatest uniformity of silicate phase distribution.

The strength of polycrystalline MgO at high temperatures has been shown to depend on the ease of dislocation motion. Yielding in specimens containing a boundary phase has been found to be related to the uniformity of distribution of that phase over a wide temperature range, and specifically to the ease of dislocation motion at 1200°C. The means by which fracture occurs at various temperatures in the specimens containing $CaO \cdot MgO \cdot SiO_2$ can be readily explained through further consideration of yielding for both MgO and MgO-$CaO \cdot MgO \cdot SiO_2$ materials.

While the yield stresses of a number of specimens containing $CaO \cdot MgO \cdot SiO_2$ were greater than the yield stresses of MgO specimens of Type I at corresponding temperatures, it has previously been noted that most of the specimens fractured at lower stresses. The MgO specimens were observed to have relatively low yield stresses, but the load-bearing capacity of the specimens increased with strain as the effects of work hardening became more pronounced. The stress at fracture was therefore much higher. The effect of work hardening is reflected in the gradual decrease in the slope of the stress-strain curves shown in Fig. 5 for Type I specimens of MgO, as noted previously. The gradual change in the slope of the stress-strain curves for materials containing $CaO \cdot MgO \cdot SiO_2$ tested at 1200°C (Figs. 11 and 14) are also indicative of work hardening, although the degree of hardening is restricted by the boundary phase and its distribution, and by yielding of the boundary due to the presence of a residual glassy phase. Consequently, the specimens containing $CaO \cdot MgO \cdot SiO_2$ generally fracture at lower stress levels than the MgO specimens of Type I, and the total strain at fracture is much less. When the increase in the yield strength due to the presence of the



silicate phase is great (i.e., for the Type I 15% specimen and the Type II 5% specimen), however, it was observed that the strength at fracture may approach and even exceed that of pure MgO, although the total strains at fracture are much different. The total strains recorded for all specimens up to the point of fracture are included in Tables III and IV.

At higher temperatures fracture in specimens containing $CaO \cdot MgO \cdot SiO_2$ occurs following deformation of the boundary phase. A rapid increase in strain rate is observed following yielding in most of these materials, particularly in Type I specimens where the silicate phase is more uniformly distributed (Figs. 12 and 13). While stresses achieved in the 15% $CaO \cdot MgO \cdot SiO_2$ specimen of Type I, and in the 5% $CaO \cdot MgO \cdot SiO_2$ specimen of Type II, were sufficiently high to activate slip within the MgO grains at all temperatures studied, the stress levels achieved at 1300°C and 1400°C for all other specimens containing $CaO \cdot MgO \cdot SiO_2$ were too low to cause extensive dislocation motion. Viscous deformation of the silicate phase along grain boundaries resulted in cavitation and fracture at low stresses.

For all specimens containing $CaO \cdot MgO \cdot SiO_2$ fracture was observed to be intergranular. However, examination of the fracture surface shown in Fig. 17 for the Type II specimen containing 5% $CaO \cdot MgO \cdot SiO_2$ tested at 1200°C indicates some evidence of transgranular fracture. It is suggested that this must result from deformation within individual grains of MgO at stresses high enough to activate slip, even though the boundary phase restricts the total amount of plastic straining possible before fracture.

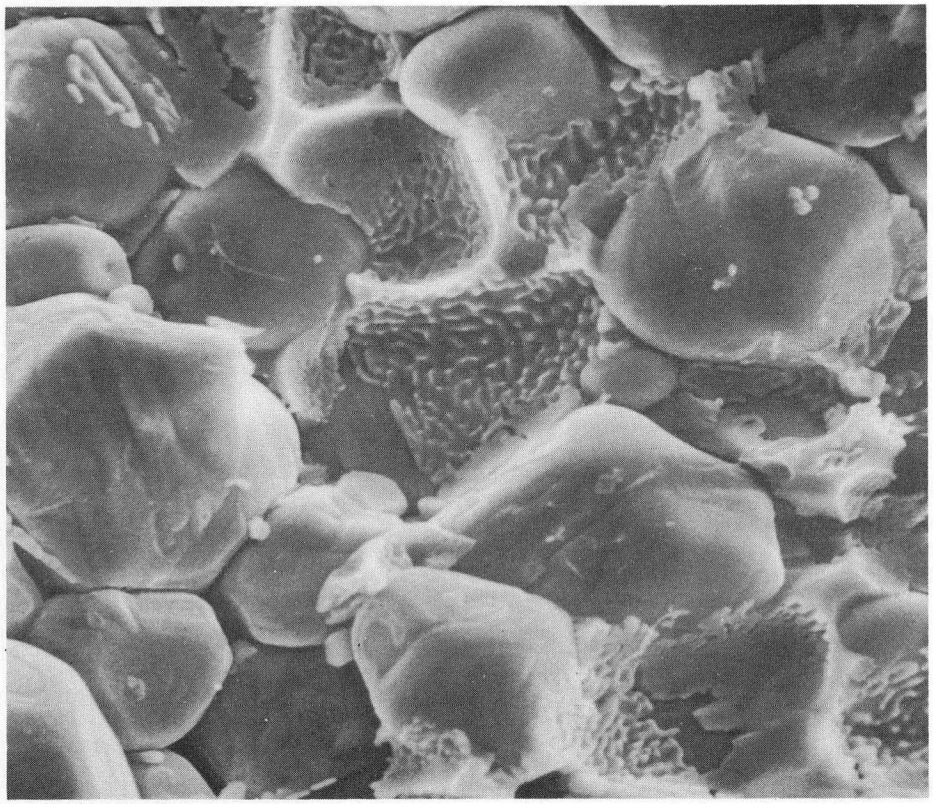

XBB 715-2112

Figure 17. Scanning electron micrograph of the fracture surface of a Type II specimen containing 5% $CaO \cdot MgO \cdot SiO_2$ strained 2.5% at 1200°C. 1200X



## C. Creep

Creep tests for Type II specimens containing 5% $CaO \cdot MgO \cdot SiO_2$ were conducted over the temperature range 1200°C-1450°C. The tests were designed to give creep rates in the steady-state region of deformation of approximately $10^{-7}$/sec. Thus as the test temperature was increased, the stresses applied were reduced some predetermined amount. Creep curves which illustrate the behavior of these specimens at several temperatures are presented in Fig. 18.

At 1200°C, the initial elastic extension accompanying application of the load was small, and it was difficult to distinguish a region of primary creep. For strains greater than approximately 1%, the strain rate remained constant during the remainder of the test. At 1300°C, a relatively long primary region was observed and steady-state creep was not established until the strain reached approximately 7%. At 1400°C a primary region of intermediate length (up to 2% strain) was observed before the creep rate became constant.

Following the establishment of the initial steady-state in a number of separate tests, the stress was changed and a new steady-state creep rate was determined. A number of such incremental changes in stress were made at temperatures of 1200°C, 1300°C, 1400°C, and 1450°C to obtain data for the steady-state creep rate as a function of stress at a given temperature. This data was used to calculate the stress exponent n discussed in Section II-B.

The value for the stress exponent at each temperature was determined using a modified form of Eq. (3). The equation as presented was derived for conditions where dislocation processes are likely to dominate creep behavior. However, for the specimens containing $CaO \cdot MgO \cdot SiO_2$ studied in this work, stress-strain results have shown that the effects of

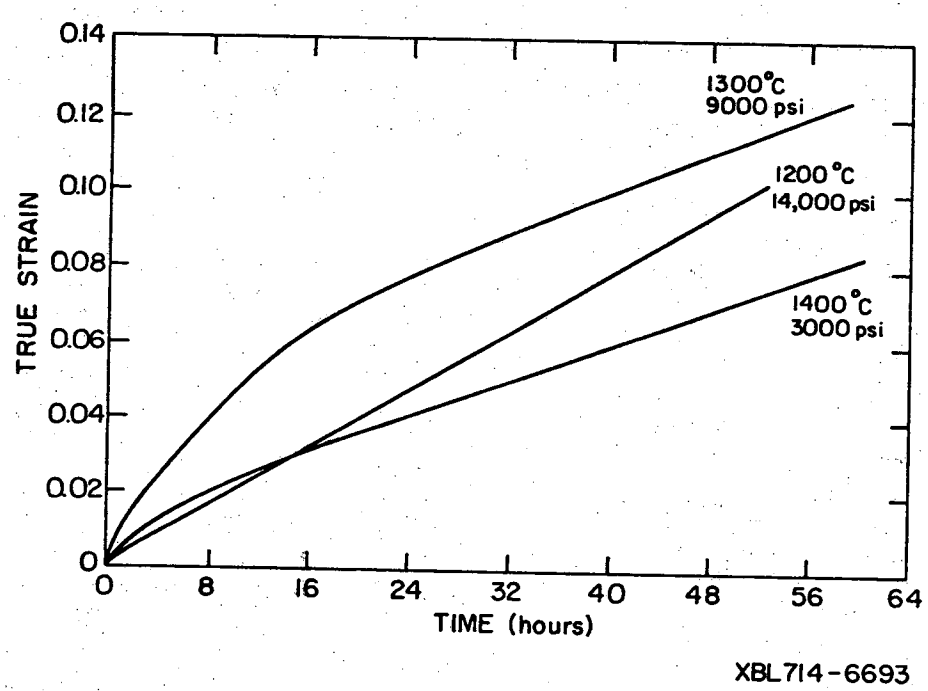


Figure 18. Typical creep curves for Type II specimens containing 5% $CaO \cdot MgO \cdot SiO_2$.



dislocation motion on deformation are significantly reduced as the temperature is increased and the boundary phase controls deformation. Under these conditions it seems that including the Burgers vector b in the creep rate equation is not meaningful. Perhaps some other value for length such as the width of the boundary phase should be substituted at higher temperatures. Furthermore, Eq. (3) was formulated for single phase materials for which the shear modulus G is easily determined. In the system being investigated, it is probably preferable to use values for the shear modulus of the second phase as a function of temperature. However, these values are not known, and they cannot be calculated with any degree of certainty.

To overcome the uncertainty expected in values for G and boundary width at various temperatures, a number of parameters were combined to give a single temperature dependent constant A' which could be determined experimentally. Thus creep in the 5% $CaO \cdot MgO \cdot SiO_2$ specimen of Type II can be described as

$$\dot{\varepsilon} = A'\left(\frac{\sigma}{G}\right)^n e^{-Q/RT} \qquad (7)$$

where A' has dimensions of $(\text{time})^{-1}$. Q represents the apparent activation energy for creep determined at the temperature T. The shear modulus to be substituted in Eq. (7) was that for dense polycrystalline MgO. Using the room temperature data of Janowski and Rossi,[54] the shear modulus at various temperatures was calculated using the relation

$$G_T/G_{298} = 1.065 - 1.98 + 10^{-4}\ T \qquad (8)$$

determined by Soga et al.[55] $G_T$ and $G_{298}$ represent the shear modulus at

the temperatures T and 298°K, respectively.

Experimental values for the strain rate as a function of $\sigma/G$ for four different temperatures have been plotted in Fig. 19. From Eq. (7), it is seen that the relation

$$\log \dot{e} = n \log\left(\frac{\sigma}{G}\right) + \log\left(A' e^{-Q/RT}\right) \qquad (9)$$

represents a straight line with slope n and intercept $\log\left(A' e^{-Q/RT}\right)$. From a least squares analysis of the data obtained at each temperature values for n and $A' e^{-Q/RT}$ were easily determined.

The apparent activation energy for creep was determined at several temperatures in the range 1200-1450°C using an incremental temperature technique, as noted in Section III-C. The steady-state creep rate of a specimen subjected to a constant stress was determined following incremental temperature changes of ± 20°C. For example, the apparent activation energy for creep at 1300°C was determined from data obtained by periodic cycling between 1290°C and 1310°C. The apparent activation energy Q could then be calculated using an expression derived from Eq. (3):

$$Q = \frac{R \ln \dfrac{(\dot{\varepsilon}_1 T_1/G_1)}{(\dot{\varepsilon}_2 T_2/G_2)}}{1/T_2 - 1/T_1} \qquad (10)$$

where $\dot{\varepsilon}_1$ and $\dot{\varepsilon}_2$ represent the strain rate at temperatures $T_1$ and $T_2$, respectively, and $G_1$ and $G_2$ represent the shear modulus at the corresponding temperatures. Although precise values for $G_1$ and $G_2$ were not known, it was assumed that they were approximately the same for the small temperature change. The ratio $T_1G_2/T_2G_1$ was thus considered to be



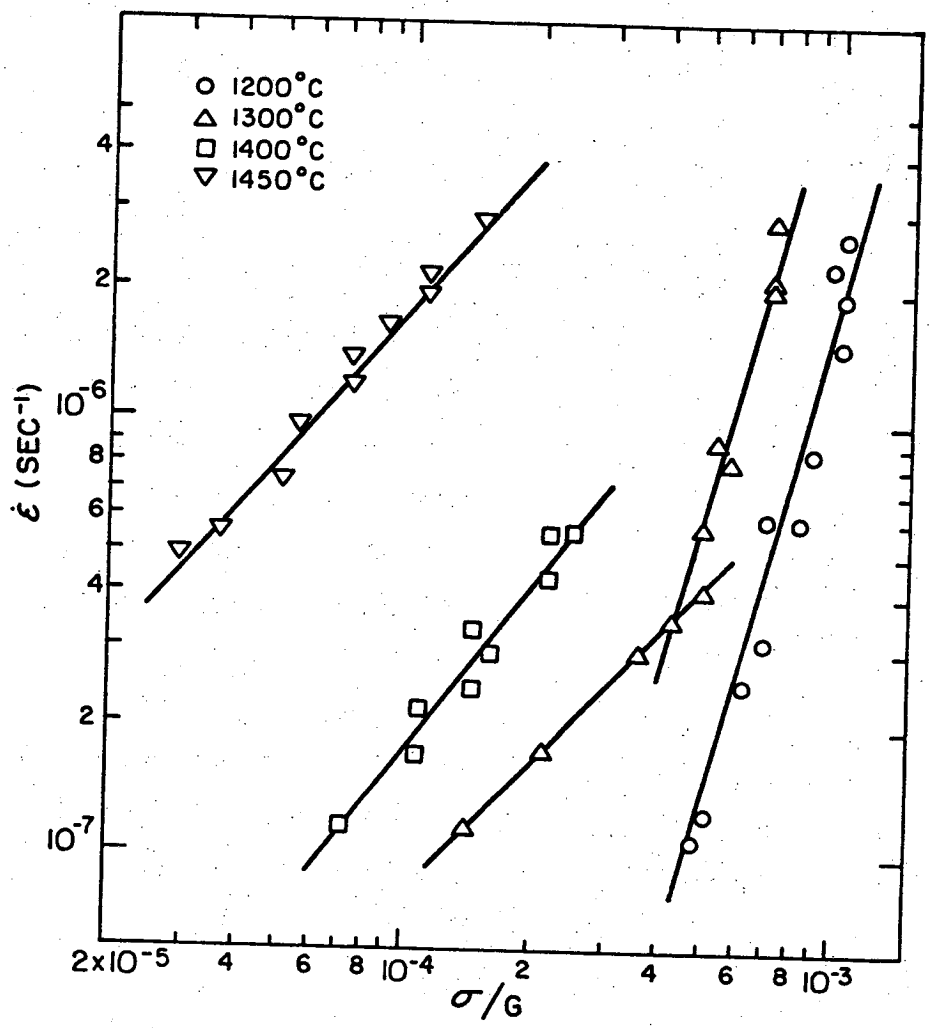


XBL714-6692

Figure 19. Strain-rate vs. normalized stress for creep specimens (5% $CaO{\cdot}MgO{\cdot}SiO_2$) tested in the temperature range 1200-1450°C.

equal to one, and the apparent activation energy was actually determined from the relation

$$Q = \frac{R \ln \dot{\varepsilon}_1/\dot{\varepsilon}_2}{\frac{1}{T_2} - \frac{1}{T_1}} \qquad (11)$$

This result can also be determined directly from Eq. (7) assuming that the temperature dependent constant A' is not significantly affected by a 20°C change.

An average value obtained from several calculations was determined for Q at each temperature. This value was then used to calculate the constant A', where $A'e^{-Q/RT}$ was known from the least squares analysis of the data shown in Fig. 19.

Values for the stress exponent n, the apparent activation energy for creep Q, and A' are presented in Table V. In general, it was found that the stress exponent n decreased as the temperature was increased. The apparent activation energy for creep, however, was found to increase with temperature. Both of these results were consistent with expectations of a changing deformation mechanism with temperature for the specimens.

Table V. Calculated and experimental values for the parameters in the creep equation (Eq. 7)

| Temperature | $G_T$ | n | Q | A' |
|---|---|---|---|---|
| 1200°C | $14.6 \times 10^6$ psi | 3.62 | 104 kcal/mole | $3.26 \times 10^{20}$/sec |
| 1300°C | $14.2 \times 10^6$ psi | | | |
| $\sigma > 7000$ psi | | 3.81 | 130 kcal/mole | $2.71 \times 10^{24}$ |
| $\sigma < 7000$ psi | | 1.01 | 130 kcal/mole | $1.06 \times 10^{15}$ |
| 1400°C | $13.8 \times 10^6$ psi | 1.30 | 215 kcal/mole | $3.33 \times 10^{26}$/sec |
| 1450°C | $13.6 \times 10^6$ psi | 1.13 | 240 kcal/mole | $1.76 \times 10^{29}$/sec |



At 1200°C the stress exponent n was found to be 3.6, indicating that deformation may have been the result of some dislocation controlled process. The value noted is consistent with the predictions by Weertman[16] of stress exponenets between 3 and 4 for creep occurring as a result of dislocation climb. This result is also in good agreement with the value for n of 3.3 determined by Langdon and Pask[32] for compressive creep of polycrystalline MgO at 1200°C, where deformation was concluded to be due to some form of dislocation motion.

The apparent activation energy for creep at 1200°C was found to be 104 kcal/mole. While this value is much higher than the values determined by Langdon and Pask[32] for creep of MgO at 1200°C, or by Oishi and Kingery[26] for diffusion of oxygen in MgO, it is in good agreement with the results of Hensler and Cullen[29] (111 ± 12 kcal/mole), and Tagai and Zisner[31] (104-106 kcal/mole), for creep of polycrystalline specimens. Hensler and Cullen[29] have noted that the value determined by Oishi and Kingery may be too low to correspond to oxygen lattice diffusion in high purity MgO. Furthermore, recent work by Narayan[56] suggests that the value determined by Oishi and Kingery must actually represent the activation energy for (extrinsic) boundary diffusion. Narayan observed the shrinkage of dislocation dipoles in thin foils of MgO using transmission electron microscopy and determined the activation energy for pipe diffusion (diffusion along the core of a dislocation) to be 60.4 kcal/mole, which compares favorably to the value of 62.4 kcal/mole reported by Oishi and Kingery. In a similar investigation, the activation energy for bulk diffusion of oxygen in MgO was found to be 110 kcal/mole.[57] This result is in excellent agreement with the value determined from creep data in this work, and also with a value of 120 kcal/mole for the activation energy for intrinsic diffusion of oxygen in

polycrystalline MgO determined by electrical conductivity measurements.[58]

Further evidence that creep at 1200°C in the Type II specimens containing 5% $CaO \cdot MgO \cdot SiO_2$ must be controlled by deformation within the MgO framework is provided in Fig. 20. The photomicrograph of a specimen strained approximately 10% at 1200°C reveals no deformation in the boundary phase. The specimen is similar in appearance to the undeformed specimen shown in Fig. 2. Since deformation occurring by some dislcoation process within individual MgO grains requires a change in grain shape, the boundary phase must undergo limited deformation to maintain the integrity of the MgO-silicate interfaces.

At 1300°C the stress exponent n was found to have two distinct values, as indicated in Fig. 19. For higher levels of stress (>7000 psi) the stress exponent was found to be 3.8, or essentially the same as that determined at 1200°C. For lower values of stress a stress exponent of 1.0 was found. The two values for n indicate that at 1300°C a second deformation mechanism begins to play a significant role in the creep of $MgO-CaO \cdot MgO \cdot SiO_2$ specimens. This may contribute to the long primary region for creep at 1300°C shown in Fig. 18. The level of stress (7000 psi) in the region of transition is approximately equal to the yield stress of Type I specimens of MgO at 1300°C. It is also in good agreement with an average yield stress for MgO single crystals determined from the results of Copley and Pask[8] for <100> and <111> stress axes. These observations suggest that at higher stresses the creep of $MgO-CaO \cdot MgO \cdot SiO_2$ specimens at 1300°C is controlled by dislocation processes similar to those determined to be rate-controlling at 1200°C. At lower stresses the stress exponent of 1.0 suggests that deformation might be the result of a viscous mechanism, such as diffusion controlled creep required for the Nabarro-Herring,[20] Coble,[21] or Gifkins[24] models.



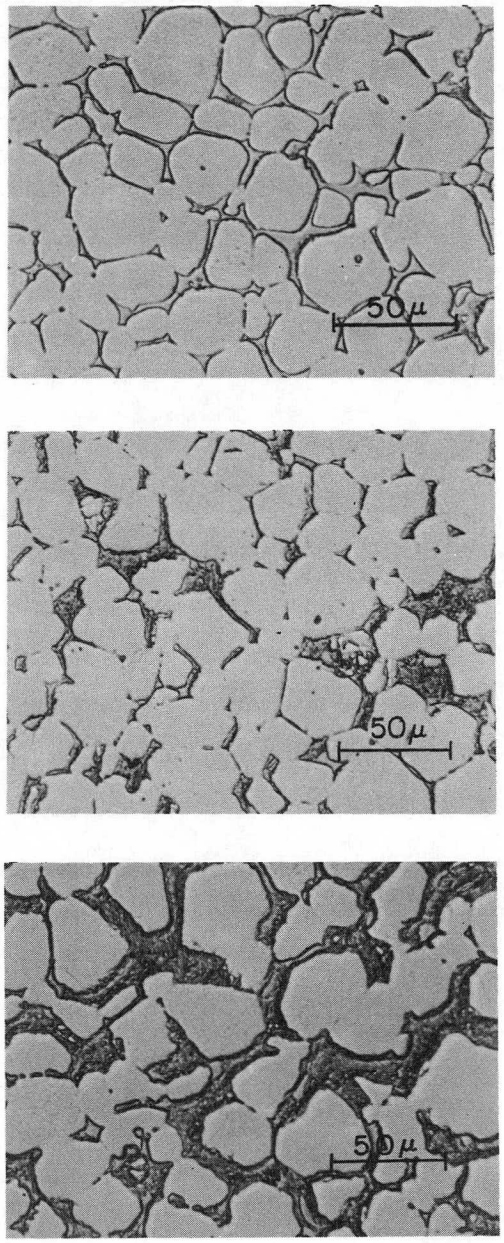


~10% strain 1200°C

~12% strain 1300°C

~10% strain 1400°C

XBB 715-2117

Figure 20. Photomicrographs of specimens containing 5% $CaO \cdot MgO \cdot SiO_2$ strained 10-12% in creep tests. Sections normal to the loading axis.

It is also possible, however, that the linear dependence of strain rate on stress in this range is due to viscous deformation of the boundary phase, with the sliding involved subject to a Newtonian viscosity law and not dependent on any diffusion process. Ke[59] has shown that grain boundaries under shear stresses behave viscously with strain rate linearly proportional to stress. Examination of the photomicrograph shown in Fig. 20 for a specimen deformed 12% at 1300°C in an incremental stress test indicates some evidence of deformation in the boundary phase. The absence of cracks caused by grain boundary separation may be interpreted as evidence of actual flow of the silicate phase. Therefore, creep at 1300°C in specimens containing $CaO \cdot MgO \cdot SiO_2$ is probably the result of viscous flow of the boundary phase when the stresses are too low to activate slip within MgO grains.

The apparent activation energy for creep at 1300°C was determined to be 130 kcal/mole. This value was found to be independent of stress in the range 6000-10,000 psi, although the range includes the region of transition from a dislocation mechanism to a sliding mechanism during creep. The significance of a change in the apparent activation energy for creep as a result of a change in the mechanism controlling deformation has been discussed by Langdon.[23] Although a single mechanism is usually rate controlling, if two or more mechanisms operate they may act either sequentially or simultaneously. If two mechanisms operating sequentially have different activation energies, there is a change in the apparent activation for creep from a high value to a low value as the temperature is increased. If the two mechanisms operate simultaneously, however, the change in the apparent activation energy for creep is from a lower value to a higher value as the temperature is increased. Thus the increase in the apparent activation energy for



creep noted for specimens containing $CaO \cdot MgO \cdot SiO_2$ indicates that the two deformation mechanisms must operate simultaneously at stresses high enough to promote slip within the MgO grains.

It is of interest to note that when the stress exponent n for creep at 1300°C was obtained using Eq. (2) an intermediate value of n was found. Values for $\log \dot{\varepsilon}_2/\dot{\varepsilon}_1$ vs. $\log \sigma_2/\sigma_1$ were plotted, where the ratios represent the observed change in strain rate accompanying a change in stress in an incremental stress test. The effect of stress on the mechanism controlling creep at 1300°C so evident in Fig. 19 was not detected and an average value for n of 2.8 was determined. The more direct method of plotting $\log \dot{\varepsilon}$ vs. $\log \left(\frac{\sigma}{G}\right)$ as in Fig. 19 was thus found to give a much clearer indication of the deformation processes taking place.

At 1400°C and 1450°C the stress exponents were found to be 1.3 and 1.1, respectively. This indicates that at these temperatures deformation is largely the result of viscous flow of the boundary phase. Similar values for n of 1.2 and 1.1 for creep of MgO containing LiF as a liquid phase have been reported.[60] Creep was concluded to be the result of Newtonian or pseudo-Newtonian deformation of the LiF boundary phase. Evidence of such deformation in the $MgO-CaO \cdot MgO \cdot SiO_2$ specimens is revealed in the photomicrograph of Fig. 20 for a specimen deformed 10% at 1400°C. The flow of the boundary phase is seen to be extensive. It should be noted that this photomicrograph represents an area perpendicular to the loading axis in a region close to the center of the specimen where the local strains are expected to be greatest. In regions of the specimen closer to the edges, the extent of viscous flow of the boundary phase was not as great. As in the specimens tested at 1300°C, no evidence of crack formation was observed. It was not

possible at these temperatures to raise the stress to levels high enough to activate slip within the MgO grains since the creep rate became very rapid for stresses above approximately 5000 psi at 1400°C and 3500 psi at 1450°C and the specimens soon fractured.

The apparent activation energy for creep at 1400°C was found to be 215 kcal/mole. At 1450°C this value increased to 240 kcal/mole. Although these values are quite high relative to the value obtained at 1200°C, comparable values have been reported for the apparent activation energy of magnesia firebricks deforming in the presence of a liquid phase.[40]

To check the values reported in Table V for the apparent activation energy for creep obtained using data from incremental temperature tests, data from other tests were considered. Using strain-rate data presented in Fig. 19, the apparent activation energy was calculated from Eq. (10) assuming a constant value for the shear modulus. At a stress of 10,000 psi, and using strain rate data at 1200°C and 1300°C, the apparent activation energy in the region where dislocation mechanisms were found to control creep was determined to be between 90 kcal/mole and 105 kcal/mole. This is in good agreement with the value of 104 kcal/mole obtained using the incremental temperature data. At a stress of 2000 psi, and using values for the strain rate at 1400°C and 1450°C, the apparent activation energy for creep was calculated to be approximately 250 kcal/mole. This value is also in good agreement with values obtained at 1400°C and 1450°C using the incremental temperature data, where it was determined that the creep process was controlled by viscous deformation of the boundary phase.

Values for Q obtained using strain-rate data at 1300°C (lower stresses) and 1450°C were lower than expected. This must be due to the



great differences in the structures of the material at the two temperatures, i.e., the shear modulus of the boundary phase must change appreciably over the indicated temperature range. The lower values for the activation energy calculated from this data, then, suggest that the error is due not to the particular data used but rather to the incorrect assumption that G remained constant over such a large temperature range. Thus the incremental temperature technique appears to be a valid means of obtaining reasonable values for the apparent activation energy for creep.

## V. SUMMARY AND CONCLUSIONS

Specimens of polycrystalline MgO containing up to 15% of a silicate phase were fabricated by vacuum hot pressing or hot pressing and annealing techniques. The silicate phase was distributed along MgO grain boundaries, and consisted of crystalline $CaO \cdot MgO \cdot SiO_2$ (monticellite) and small amounts of a residual glassy phase.

The high temperature mechanical behavior of these specimens in stress-strain tests was studied over the temperature range 1200-1400°C. The mechanical behavior was found to be dependent on the degree of uniformity of distribution of the boundary phase, particularly at 1200°C. At this temperature deformation occurred primarily as the result of plastic deformation in the MgO framework. At higher temperatures deformation was controlled by deformation within the silicate phase as additional softening of the residual glassy phase occurred. At all temperatures the most favorable mechanical behavior was exhibited by those specimens having the most uniform distribution of the boundary phase. The behavior of Type I specimens containing 15% $CaO \cdot MgO \cdot SiO_2$ was found to be essentially the same as that of Type II specimens containing only 5% $CaO \cdot MgO \cdot SiO_2$ where the amount of MgO grain-grain contact area was approximately equivalent for each type.

The importance of the strength of grain boundaries in determining the high temperature mechanical behavior of polycrystalline MgO was studied in other experiments. Specimens hot pressed at 1450°C exhibited relatively high strengths but limited ductility in the temperature range 1200-1400°C. Similar specimens which had also been annealed at 1550°C yielded at much lower stress levels but exhibited a significant amount of plastic deformation as a result of dislocation motion before fracture.



Results of creep tests for specimens containing ∿5% $CaO \cdot MgO \cdot SiO_2$ uniformly distributed have shown that at 1200°C deformation occurs as a result of dislocation processes, such as dislocation climb. The stress exponent at 1200°C was found to be 3.6. The apparent activation energy for creep, determined using an incremental temperature technique, was 104 kcal/mole. This value is in good agreement with a number of values reported for creep of polycrystalline MgO, as well as for the bulk diffusion of oxygen in MgO recently determined.

Creep at 1300°C was found to occur as a result of two deformation mechanisms. At higher stresses creep was controlled by dislocation processes, and a stress exponent of 3.8 was noted. At lower stresses creep was controlled by viscous flow of the boundary phase and a value of 1.0 was determined for the stress exponent. The apparent activation energy for creep at 1300°C was 130 kcal/mole. The increase in activation energy with temperature was consistent with expectations that such an increase should be observed where two mechanisms affecting deformation operate simultaneously.

At 1400°C and 1450°C creep of specimens containing ∿5% $CaO \cdot MgO \cdot SiO_2$ occurred as a result of viscous flow of the boundary phase. The stress exponents were found to be 1.3 and 1.1 at these temperatures, respectively. The apparent activation energy for creep was greater than 200 kcal/mole.

To check the values reported for the apparent activation energy for creep determined using an incremental temperature technique, data from other tests were considered. For creep occurring as a result of dislocation processes the apparent activation energy was calculated to be ∿100 kcal/mole. The activation energy for viscous flow of the boundary phase was calculated to be ∿250 kcal/mole. Thus the

incremental temperature technique appears to be a valid means of determining reasonable values for the apparent activation energy for creep.



## ACKNOWLEDGMENTS

The author wishes to thank Professor Joseph A. Pask for his guidance during the course of this investigation. The technical assistance of Donald R. Cropper, Neal Houlding, Gloria Pelatowski, and Kelly Radmilovic was also greatly appreciated.

Special thanks are extended to the Foundation in Refractories Education for providing generous financial support, and to James C. Hicks of Kaiser Refractories, whose continued interest in this work was most encouraging.

This work was done under the auspices of the United States Atomic Energy Commission.

# APPENDIX

## 1. The Chemical Analysis of MgO Powder

Baker and Adamson Reagent No. 1917

| Substance | Wt. % |
|---|---|
| Assay (MgO) (after ignition) | 99.0 |
| Insoluble in dilute HCl | 0.020 |
| Soluble in water | 0.40 |
| Loss on ignition | 2.0 |
| Ammonium hydroxide precipitate | 0.020 |
| Chloride (Cl) | 0.010 |
| Nitrite ($NO_3$) | 0.005 |
| Sulfate and sulfite (as $SO_4$) | 0.005 |
| Barium (Ba) | 0.005 |
| Calcium (Ca) | 0.05 |
| Heavy metals (as Pb) | 0.003 |
| Iron (Fe) | 0.010 |
| Manganese (Mn) | 0.0005 |
| Potassium (K) | 0.005 |
| Sodium (Na) | 0.50 |
| Stronium (Sr) | 0.005 |
| Silica ($SiO_2$) | 0.040 |



## 2. The Chemical Analysis of $CaCO_3$ Powder

Baker and Adamson Reagent No. 1506

| Substance | Wt. % |
|---|---|
| Assay ($CaCO_3$) | 99.0 |
| Insoluble in dilute HCl | 0.010 |
| $NH_4OH$ precipitate | 0.010 |
| Chloride (Cl) | 0.001 |
| Oxidizing substance (as $NO_3$) | 0.005 |
| Sulfate ($SO_4$) | 0.010 |
| Ammonium ($NH_4$) | 0.003 |
| Barium (Ba) | 0.005 |
| Stronium (Sr) | 0.10 |
| Magnesium (Mg) | 0.02 |
| Potassium (K) | 0.01 |
| Sodium (Na) | 0.10 |
| Heavy metals (as Pb) | 0.001 |
| Iron (Fe) | 0.002 |

## 3. $SiO_2$ Powder

Ottawa Silica Flour

| Substance | Wt. % |
|---|---|
| Silica ($SiO_2$) | 99.8 |
| Alumina ($Al_2O_3$) | 0.1 |
| Iron oxide ($Fe_2O_3$) | 0.02 |
| Calcium oxide and magnesium oxide (CaO, MgO) | 0.1 |

## REFERENCES


1. C. O. Hulse, S. M. Copley, and J. A. Pask, "Effect of Crystal Orientation on Plastic Deformation of Magnesium Oxide," J. Am. Ceram. Soc., 46 [7] 317-322 (1963).
2. A. E. Gorum, E. R. Parker, and J. A. Pask, "Effect of Surface Conditions on Room Temperature Ductility of Ionic Crystals," J. Am. Ceram. Soc., 41 [5] 161-164 (1958).
3. R. J. Stokes, T. L. Johnston, and C. H. Li, "Crack Formation in Magnesium Oxide Single Crystals," Phil. Mag. [8], 3 [31] 718-25 (1958).
4. C. O. Hulse and J. A. Pask, "Mechanical Properties of Magnesia Single Crystals in Compression," J. Am. Ceram. Soc., 43 [7] 373-78 (1960).
5. J. E. May and M. L. Kronberg, "Temperature Dependence of Plastic Yield Stress of Single Crystals of Magnesium Oxide," J. Am. Ceram. Soc., 43 [10] 525-30 (1960).
6. A. E. Gorum, W. J. Luhman, and J. A. Pask, "Effect of Impurities and Heat Treatment on Ductility of MgO," J. Am. Ceram. Soc., 43 [5] 241-245 (1960).
7. R. B. Day and R. J. Stokes, "Mechanical Behavior of Magnesium Oxide at High Temperatures," J. Am. Ceram. Soc., 47 [10] 493-503 (1964).
8. S. M. Copley and J. A. Pask, "Plastic Deformation of MgO Single Crystals up to 1600°C," J. Am. Ceram. Soc., 48 [3] 139-146 (1965).
9. R. J. Stokes and C. H. Li, "Dislocations and the Tensile Strength of Magnesium Oxide," J. Am. Ceram. Soc., 46 [9] 423-434 (1963).
10. T. Vasilos, J. B. Mitchell, and R. M. Spriggs, "Mechanical Properties of Pure, Dense Magnesium Oxide as a Function of Temperature and Grain Size," J. Am. Ceram. Soc., 47 [12] 601-610 (1964).





11. R. B. Day and R. J. Stokes, "Mechanical Behavior of Polycrystalline Magnesium Oxide at High Temperatures," J. Am. Ceram. Soc., 49 [7] 345-354 (1966).
12. S. M. Copley and J. A. Pask, "Deformation of Polycrystalline MgO at Elevated Temperatures," J. Am. Ceram. Soc., 48 [12] 636-642 (1965).
13. A. G. Evans, D. Gilling, and R. W. Davidge, "The Temperature-Dependence of the Strength of Polycrystalline MgO," J. Matl. Sci., 5 (1970) 187-197.
14. T. G. Langdon and J. A. Pask, "Mechanical Behavior of Single Crystal and Polycrystalline MgO," UCRL-18250, University of California, June 1968.
15. A. K. Mukherjee, J. E. Bird and J. E. Dorn, "Experimental Correlations for High Temperature Creep," UCRL-18526, University of California, Berkeley, Oct. 1968.
16. J. Weertman, "Theory of Steady-State Creep Based on Dislocation Climb," J. Appl. Phys., 26 [10] 1213 (1955).
17. J. Weertman, "Steady-State Creep Through Dislocation Climb," J. Appl. Phys. 28 [3] 362-364 (1957).
18. F. R. N. Nabarro, "Steady-State Diffusional Creep," Phil. Mag. 16 [140] 231-237 (1967).
19. F. R. N. Nabarro, "Report of a Conference on the Strength of Solids," (Physical Society, London, 1948). p. 75.
20. C. Herring, "Diffusional Viscosity of a Polycrystalline Solid," J. Appl. Phys., 21 [5] 437-445 (1950).
21. R. L. Coble, "A Model for Boundary Diffusion Controlled Creep in Polycrystalline Materials," J. Appl. Phys. 34 [6] 1679-1682 (1963).

22. J. E. Bird, A. K. Mukherjee, and J. E. Dorn, "Correlations Between High Temperature Creep Behavior and Structure," UCRL-19056, University of California, July 1969.

23. T. G. Langdon, "Grain Boundary Sliding as a Deformation Mechanism During Creep," Phil. Mag., 22 [178] 689-700 (1970).

24. R. C. Gifkins, "Diffusional Creep Mechanisms," J. Am. Ceram. Soc., 51 [2] 69-71 (1968).

25. T. Vasilos, J. B. Mitchell, and R. M. Spriggs, "Creep of Polycrystalline Magnesia," J. Am. Ceram. Soc., 47 [4] 203-204 (1964).

26. Y. Oishi and W. D. Kingery, "Oxygen Diffusion in Periclase Crystals" J. Chem. Phys., 33 [3] 905-906 (1960).

27. E. M. Passmore, R. H. Duff, and T. Vasilos, "Creep of Dense, Polycrystalline Magnesium Oxide," J. Am. Ceram. Soc., 49 [11] 594-600 (1966).

28. J. H. Hensler and G. V. Cullen, "Grain Shape Change During Creep in Magnesium Oxide," J. Am. Ceram. Soc., 50 [11] 584-585 (1967).

29. J. H. Hensler and G. V. Cullen, "Stress, Temperature, and Strain Rate in Creep of Magnesium Oxide," J. Am. Ceram. Soc., 51 [10] 594-599 (1968).

30. H. Tagai and T. Zisner, "High-Temperature Creep of Polycrystalline Magnesia: I, Effect of Simultaneous Grain Growth," J. Am. Ceram. Soc., 51 [6] 303-310 (1968).

31. T. Zisner and H. Tagai, "High-Temperature Creep of Polycrystalline Magnesia, II, Effects of Additives," J. Am. Ceram. Soc., 51 [6] 310-314 (1968).

32. T. G. Langdon and J. A. Pask, "The Mechanism of Creep in Polycrystalline Magnesium Oxide," Acta. Met., 18 May 1970 pp. 505-510.



33. A. Hayhurst and J. Laming, "The Structure of Chrome-Magnesite Refractories at High Temperatures," Trans. Brit. Ceram. Soc., 62 [12] 989-1005 (1963).

34. A. Hayhurst and J. Laming, "Modifications of Microstructure of Chrome-Magnesite Refractories by Heat Treatment," Trans. Brit. Ceram. Soc., 63 [3] 135-142 (1964).

35. T. Hatfield, C. Richmond, W. F. Ford, and J. White, "Compatability Relationship Between the Periclase and Silicate Phases in Magnesite Refractories at High Temperatures," Trans. Brit. Ceram. Soc., 69 [2] 53-58 (1970).

36. W. F. Ford, A. Hayhurst, and J. White, "The Effect of Bond Structure on the High Temperature Tensile Behavior of Basic Bricks," Trans. Brit. Ceram. Soc., 60 [8] 581-601 (1961).

37. B. H. Baker and P. Schroth, "High Hot Strength in Basic Brick," Bull. Am. Ceram. Soc., 47 [7] 623-626 (1968).

38. H. J. S. Kriek and B. B. Segal, "Effect of the Silicate Constitution of Magnesite Bricks on the High-Temperature Strength," Trans. Brit. Ceram. Soc., 66 [2] 65-83 (1967).

39. J. R. Kreglo, Jr., and W. J. Smothers, "Mechanism of Creep in MgO Brick," J. Am. Ceram. Soc., 50 [9] 457-460 (1967).

40. C. O. Hulse and J. A. Pask, "An Analysis of the Deformation of a Firebrick," Ceramic Laboratories, University of California, Berkeley, July 1962.

41. R. F. Stoops, Am. Ceram. Soc. Bull., 45 [4] 449 (1966). Paper presented at the 68th Annual Meeting of the American Ceramic Society, Washington, D.C., May 11, 1966.

42. C. O. Hulse and S. M. Copley, "High Temperature Compressive Deformation Equipment," Am. Ceram. Soc. Bull., 45 [5] 530-534 (1966).

43. J. E. Dorn, "Some Fundamental Experiments on High Temperature Creep," J. Mech. and Phys. Solids, 3 85-116 (1954).

44. W. D. Kingery, "Densification During Sintering in the Presence of a Liquid Phase. I. Theory," J. Appl. Phys., 30 [3] 301-306 (1959).

45. T. G. Sahama and K. Hytonen, "Calcium-Bearing Magnesium-Iron Olivines," Am. Min., 43 862-71 (1958).

46. D. M. Roy, "The System $Ca_2SiO_4$-$CaMgSiO_4$," Min. Mag., 31 187 (1956).

47. R. W. Ricker and E. F. Osborn, "Additional Phase Equilibrium Data for the System CaO-MgO-$SiO_2$," J. Am. Ceram. Soc., 37 [3] 133-139 (1954).

48. C. S. Smith, "Grains, Phases, and Interfaces: An Interpretation of Microstructure," Trans. AIME, 175 [1] 15-51 (1948).

49. J. White, "Phase Distribution in Ceramics," Chap. 35 in Ceramic Microstructures, ed. R. M. Fulrath and J. A. Pask, John Wiley and Sons, Inc. (1968).

50. B. Jackson, W. F. Ford, and J. White, "The Influence of $Cr_2O_3$ and $Fe_2O_3$ on the Wetting of Periclase Grains by Liquid Silicate," Trans. Brit. Ceram. Soc., 62 [7] 577-601 (1963).

51. I. M. Stephenson and J. White, "Factors Controlling Microstructure and Grain Growth in Two-Phase (One Solid + One Liquid) and in Three-Phase (Two Solid + One Liquid) Systems," Trans. Brit. Ceram. Soc., 66 [9] 443 (1967).

52. J. White, "Factors Affecting the Kinetics of Grain Growth and Densification in Ceramic Bodies Containing a Liquid Phase," Chap. 5 in Kinetics of Reactions in Ionic Systems, ed. T. J. Gray and V. D. Frechette, Plenum Press (1969).



53. D. S. Buist, B. Jackson, I. M. Stephenson, W. F. Ford, and J. White, "The Kinetics of Grain Growth in Two-Phase (Solid-Liquid) Systems," Trans. Brit. Ceram. Soc., 64 [4] 173-209 (1965).

54. K. R. Janowski and R. C. Rossi, "Elastic Behavior of MgO Matrix Composites," J. Am. Ceram. Soc. 50 [11] 599-603 (1967).

55. N. Soga, E. Schreiber, and O. L. Anderson, "Estimation of Bulk Modulus and Sound Velocities of Oxides at Very High Temperatures," J. Geophys. Res., 71 [22] 5315-5320 (1966).

56. J. Narayan, "Climb of Dislocations in Magnesium Oxide Single Crystals," UCRL-20305, University of California, Berkeley, Sept. 1970.

57. J. Narayan and J. Washburn, results to be published.

58. M. O. Davies, "Transport Phenomena in Pure and Doped Magnesium Oxide," J. Chem. Phys., 38 [9] 2047 (1963).

59. T. S. Ke, "Experimental Evidence of the Viscous Behavior of Grain Boundaries in Metals," Phys. Rev., 71 [41] 533-546 (1947).

60. P. E. Hart and J. A. Pask, "Superplasticity in the LiF-MgO System," UCRL-19699, University of California, Berkeley, Sept. 1970.

LEGAL NOTICE

*This report was prepared as an account of work sponsored by the United States Government. Neither the United States nor the United States Atomic Energy Commission, nor any of their employees, nor any of their contractors, subcontractors, or their employees, makes any warranty, express or implied, or assumes any legal liability or responsibility for the accuracy, completeness or usefulness of any information, apparatus, product or process disclosed, or represents that its use would not infringe privately owned rights.*

*TECHNICAL INFORMATION DIVISION*
*LAWRENCE BERKELEY LABORATORY*
*UNIVERSITY OF CALIFORNIA*
*BERKELEY, CALIFORNIA 94720*